Peptide Assembly Directed and Quantified Using Megadalton DNA Nanostructures

Juan Jin,[#,†] Emily G. Baker,[‡,†] Christopher W. Wood,[‡] Jonathan Bath,[#] Derek N. Woolfson,[‡,¶,§,*] and Andrew J. Turberfield[#,*]

[#]Department of Physics, Clarendon Laboratory, University of Oxford, Parks Road, Oxford, OX1 3PU, UK

[‡]School of Chemistry, University of Bristol, Cantock's Close, Bristol, BS8 1TS, UK

[¶]School of Biochemistry, Medical Sciences Building, University of Bristol, University Walk, Bristol, BS8 1TD, UK

[§]Bristol BioDesign Institute, BrisSynBio, University of Bristol Research Centre in Synthetic Biology, Life Sciences Building, Tyndall Avenue, BS8 1TQ, UK

[*]Corresponding authors: andrew.turberfield@physics.ox.ac.uk and D.N.Woolfson@bristol.ac.uk

[†]Contributed equally to this work

Table of Contents

Supporting Methods

Peptide modelling. Parametric models for all six combinations of CC-Di-EK and CC-Di-KE as hetero and homodimeric parallel and antiparallel coiled coils were generated using ISAMBARD (https://github.com/woolfson-group/isambard).[1] These were optimized for BUDE Interaction Energy in ISAMBARD using a genetic algorithm which generated 30,000 models per combination over 30 generations with 1,000 models in each. To ensure that we generated useful models, we restricted geometric parameters to values consistent with coiled-coil dimers. For both the parallel and antiparallel models these were: radius = 5.0 ± 1.0 Å, pitch = 180 ± 50 Å, φCα1 = 180 ± 10°, φCα2 = 180 ± 10°, and z shift = 0 ± 5 Å. Optimizations were repeated three times for each combination.

Peptide purification. Crude peptides were purified using a JASCO HPLC system fitted with a semi-preparative Phenomenex Luna C18 reverse phase column (5 μM particle size; 100 Å pore size; 150 x 10 mm) and linear gradients of buffer B (0.1 % TFA in MeCN) vs. buffer A (0.1 % TFA in H_2O). The identities of purified peptides were confirmed by MALDI-TOF spectroscopy using a Bruker ultrafleXtreme II instrument in reflector mode from samples co-crystallised with dihydroxybenzoic acid matrix. Exceptions were CC-Di-EK-Z and Z-CC-Di-KE, the masses of which were confirmed by infusing sample from an Advion Nanomate Triverser (Nanospray source) at 1.4 kV into a Waters Synapt G2S IMS Q-TOF mass spectrometer. Peptide purity was determined to be >95% using a JACSO HPLC system set up with an analytical reverse phase Phenomenex Kinetex C18 column (5 μM particle size; 100 Å pore size; 100 x 4.6 mm) running linear gradients of buffer B vs. buffer A.

Peptide Concentration determinations. Peptide concentrations were determined in H_2O by UV-vis absorption at 280 nm on a Nanodrop 2000 (Thermo Scientific) using the following extinction coefficients: Trp ε_{280} = 5690 M^{-1} cm^{-1} and Tyr ε_{280} = 1280 M^{-1} cm^{-1}.

Circular dichroism (CD) spectroscopy. Peptides and peptide-oligonucleotide conjugates were prepared at the desired concentration in phosphate-buffered saline (PBS) at pH 7.4 comprising Na_2HPO_4 (8.2 mM), KH_2PO_4 (1.8 mM), NaCl (137 mM) and KCl (2.7 mM) in quartz cuvettes (Starna Scientific) of appropriate path lengths. CD spectra were baseline corrected and recorded as the average of 8 scans (260 – 190 nm) on a JASCO 815 spectropolarimeter fitted with a Peltier temperature controller at 5°C, with a scanning speed of 100 nm/min, 1 nm bandwidth, 1 nm data pitch and 1 sec response time. Thermal unfolding profiles were measured by monitoring the signal at 222 nm (1 nm bandwidth) from 5 - 95°C (temperature ramp 40°C/hr) in 1°C increments. The midpoint of the transition (T_M) was determined as the maximum of the first derivative of the thermal profile to the nearest °C.

Determination of peptide K_d by thermodynamic analysis of CD data. The K_d of CC-Di-EK:KE was determined following methods described by Marky and Breslauer.[2] Thermal unfolding profiles were recorded in triplicate over a range of peptide concentrations (100 μM, 50 μM, 20 μM and 5 μM of each peptide) for CC-Di-EK with CC-Di-KE in a 1:1 ratio. A two-state transition was assumed (Equation 1), with a negligible change in heat capacity. A model describing equilibrium for a dimer formed from two non-self-interacting peptides was used (Equation 2) where: K_a = the association constant, α = fraction folded peptide, and c_t is the total peptide concentration.

$$[A] + [B] \leftrightarrow [AB] \qquad \text{(Eq. 1)}$$

$$K_a = \frac{[AB]}{[A]+[B]} = \frac{\alpha(c_t/2)}{((1-\alpha)\,(c_t/2))^2} = \frac{\alpha}{(1-\alpha)^2\,(c_t/2)} \qquad \text{(Eq. 2)}$$

At the T_M, α = 0.5 and Equation 2 reduces to:

$$K_a(T_M) = \frac{4}{c_t} = \frac{1}{K_d(T_M)} \quad \text{(Eq. 3)}$$

From measurements of $1/T_M$ vs. $\ln(c_t)$ it is possible to determine K_d at any given temperature by assuming a linear van't Hoff relationship, Equation 4 and Figure S4.

$$\frac{1}{T_M} = \frac{R}{\Delta H^\circ} \cdot \ln(c_t) + \frac{(\Delta S^\circ - R \ln 4)}{\Delta H^\circ} \quad \text{(Eq. 4)}$$

Analytical ultracentrifugation. AUC sedimentation equilibrium experiments were performed once for each peptide, or pair of peptides, at 55 μM each in PBS (110 μL) at 20°C using a Beckman XL-A ultracentrifuge at speeds ranging 44–60 krpm in increments of 4 krpm. The reference channel contained 120 μL buffer. Either a two-channel aluminium centre piece (with sapphire windows) or resin-filled epoxy centre piece (with quartz windows) was used. For the heterodimer linked by disulphide bonds formed between opposite ends of the constituent peptides, a six-channel resin-filled epoxy centre piece (with quartz windows) was used with 110 μL in each sample channel and 120 μL of buffer in the reference channels and scans recorded in 3 krpm increments from 24–39 krpm. Scans were performed across each cell at radial distances of 5.8–7.3 cm after 8 hours at each speed and then again after a further 1 hour to check the samples had reached equilibrium before moving onto the next speed. Data were fit to calculated profiles assuming single ideal species, and partial specific volumes determined using Ultrascan II (http://ultrascan2.uthscsa.edu/). 99% confidence limits were determined by Monte Carlo analyses of the fits.

Disulfide-linked dimers. The concentration of purified CC-Di-EK-C in 1 mL H_2O was determined (ε_{280} = 10,340 M^{-1} cm^{-1}) and the sample diluted 10-fold into 10 mL. Four equivalents of 2,2'-dipyridyldisulfide (DPDS) was added in 1 mL methanol and the reaction left for 1 hour under agitation. Unreacted DPDS was removed by 3 x 10 mL diethylether extractions. The aqueous fraction containing the DPDS-activated peptide was then freeze-dried before purification by RP-HPLC as above. The concentration of the purified DPDS-activated peptide was determined in H_2O and reacted with 1 equivalent of CC-Di-KE-C and 1 equivalent of C-CC-Di-KE in PBS for 3 hours under agitation. The two disulphide-linked heterodimers were purified by HPLC and their identities confirmed by Nanospray-TOF mass spectrometry.

Peptide-oligonucleotide tag conjugation. Azide-functionalized peptides (CC-Di-EK-Z, Z-CC-Di-KE) and 5´ dibenzylcyloocytne (DBCO)-functionalized DNA oligos (α, β) were conjugated in 50 mM aqueous triethylammonium acetate (TEAA) overnight at 50°C. The peptide-oligonucleotide conjugates, CC-Di-EK-α and β-CC-Di-KE, were isolated by HPLC purification using a JASCO system with a reverse-phase analytical Phenomenex Kinetex C18 column (5 μM particle size; 100 Å pore size; 100 x 4.6 mm) running a linear gradient (10 – 60%) of buffer B (100 mM TEAA in 80:20 MeCN:H_2O) vs. buffer A (100 mM TEAA in H_2O), while monitoring the absorbance at 280 and 260 nm. After freeze-drying, samples were dissolved in H_2O and desalted into water using an ÄKTAprime plus system (GE Healthcare) with a HiTrap™ desalting column (GE Healthcare) and freeze dried. Conjugates were reconstituted into H_2O, divided into aliquots and freeze dried. The stock concentration was measured with a Nanodrop 2000 spectrophotometer (Thermo Scientific) using the sum of the extinction coefficients of the peptides and their ligated oligos: CC-Di-EK-α ε_{260} = 292,955 M cm^{-1}, β-CC-Di-KE ε_{260} = 293,714 M cm^{-1}. The identities of CC-Di-EK-α and β-CC-Di-KE were confirmed by submitting samples to the LC-MS service at ATDBio Ltd (Oxford) and their purities verified by in-house analytical HPLC using the same conditions as for purification of the reaction mixtures above.

Scaffold DNA preparation. Commercial pUC19 (NEB) was transformed into NEB® 5-alpha Competent *E. coli* and double-stranded (ds) pUC19 was collected and purified with QIAGEN Plasmid Kit. Single-stranded (ss) pUC19 was prepared by sequential reaction with Nt.BspQI at 50°C and Exonuclease III at 37°C to digest the non-template strand.[3] Enzymes were removed with QIAGEN Plasmid Kit and the DNA then recovered by ethanol precipitation.

DNA origami folding. The DNA origami was assembled from a scaffold strand (ss pUC19, 60 nM) and a 5-fold excess of staple strands in 1×TE buffer (10 mM Tris, 1 mM EDTA, pH8.0) with 16 mM $MgCl_2$. The folding mixture was heated to 80°C for 5 min then cooled to 60°C at a rate of 1°C / 4 min, to 25°C at a rate of 0.5°C / 45 min, to 15°C at a rate of 1°C / 2 min and held at 15°C.

DNA origami-peptide preparation. Assembled, unpurified DNA origami with an appropriate number of handles (approx. 60 nM) was mixed with a 3× excess of corresponding peptide-oligonucleotide conjugate and incubated at room temperature (approx. 20°C) for 2 hours.

Gel purification. The assembled origami-peptide nanostructures were purified by agarose gel electrophoresis using 0.8% agarose gel containing 0.5xTBE buffer (44.5 mM Tris, 44.5 mM boric acid, 1 mM EDTA, pH 8.3), 11 mM $MgCl_2$ at 60 V for 2-3 hours in a gel tank incubated in an ice-water bath. Target bands were cut out and squeezed on Parafilm® M. The concentration of the collected solution was determined by measuring ultraviolet absorbance at 260 nm (Cary 50 Probe UV-Visible Spectrophotometer, Varian). We assumed the extinction coefficient of the origami to be equal to that of double-stranded pUC19 (4.24×10^7 M^{-1} cm^{-1}).[4]

DNA origami-peptide assembly. Gel-purified, peptide-functionalized DNA origamis of different initial concentrations (Table S4) were mixed at room temperature (approx. 20°C) and incubated for at least 2 hours to equilibrate.

Transmission electron microscopy. DNA origami-peptide assemblies prepared as described above were adsorbed onto glow-discharged Formvar & heavier carbon film TEM grids (Agar Scientific) and then stained using 2% aqueous uranyl acetate. Imaging was performed using an FEI Tecnai T12 Transmission Electron Microscope operated at 120 kV.

Supporting Discussion

The following is an analysis of random and systematic errors in the calculation of dissociation constants based on analysis of counted numbers of origami monomers, dimers and higher multimers in transmission electron micrographs.

Concentration measurement errors
Stock origami concentrations were calculated from their absorbance at 260 nm measured using a Cary 50 Probe uv-visible spectrophotometer (Varian). The molar extinction coefficients of the two origami nanostructures were assumed to be equal to that of double-stranded pUC19 (4.24×10^7 M^{-1} cm^{-1}). The standard deviation (SD) of absorbance measurements performed in triplicate was typically <8%. The inferred concentrations of all species were scaled from these measurements: we assume a corresponding random fractional error $\delta_c = 0.08$ in the concentrations of all species.

All concentrations in a given experiment were scaled from the measured total concentration of origami A (see note on equilibrium concentration calculation in below). The fractional random error in [A]×[B]/[A:B] due to uncertainties in the measurements of origami concentrations is therefore equal to the fractional random error in $[A]_{tot}$, δ_c. Correlation between concentration errors in a given experiment was ignored in the error analysis presented below: this slightly increases the inferred error in K_d.

Sampling bias, relative abundances
Longer staining times were used for lower-concentration samples to ensure adequate densities of imaged particles. We found no systematic variation of calculated K_d with staining time.

Particle densities vary on an EM grid, therefore several locations were sampled in each experiment to maximize consistency of sampling.

Although we used nominally equal concentrations of the two peptide-decorated origamis A_n and B_n, the total numbers of B_n counted are systematically 20%±13% higher than A_n (the quoted uncertainty is the standard deviation of 24 pairs of measurements). This may reflect a sampling bias – B_n sticks to the TEM grid more readily than A_n – or a hypochromic correction to DNA absorbance at 260 nm that depends on the sub-wavelength-scale origami structure. We have assumed that the total counted number of each species (A_n or B_n) is proportional to its total concentration and have scaled the concentrations of all species in a given experiment to the measured total concentration of origami A. Uncertainty in this correction leads to a systematic error of approximately 20% in all K_ds.

Statistical sampling errors
For each system (0/1/2/3 peptides per origami) and each experiment (different initial concentrations), the total numbers of origamis A_n and B_n counted were similar (in the range 538-2137) while the counted numbers of homo- and heterodimers varied greatly. We estimate the standard error of the total number of each species 'x' in a sample as the square root of the number N_x counted. The corresponding fractional random error in the inferred concentration is $(N_x)^{-0.5}$.

Identification errors
Species were identified and counted by eye. We estimate that errors due to misidentification of origami A as B and vice versa were small compared to statistical sampling errors. Some species identified as peptide-linked dimers are, in fact, unlinked pairs of monomers whose functionalized ends lie, by chance, close to each other. Dimers are thus overcounted.
Each electron micrograph is square of side L = 2 μm. Let t be the tolerance for judging whether two origamis are actually connected, *i.e.*, pairs of origamis whose peptide-functionalized ends are separated by a distance less than t are identified as dimers whether or not they are physically linked (we estimate that t is approximately 10 nm). The number of false positives (FP) per micrograph is therefore $N_A N_B / n_m^2 \times \pi t^2 / L^2$ (heterodimer) or $N_x^2 / (2n_m^2) \times \pi t^2 / L^2$ (homodimer), where N_X is the total number of

origamis of type X counted in n_m micrographs. The corresponding total numbers of false positives in each experiment is $N_{FP} = N_A N_B / n_m \times \pi t^2 / L^2$ (heterodimer) or $N_x^2 / (2n_m) \times \pi t^2 / L^2$ (homodimer).

If we assume that there is no significant association between origamis with no linking peptides attached, *i.e.*, all dimers counted in such experiments are 'false positives', then we obtain from these data an improved estimate of the range parameter t = 8±1 nm. (There is a small but significant systematic difference between values of t calculated for hetero- and homo-dimeric complexes which may reflect a real attractive interaction between the ends of linked origamis.) We use this estimate to calculate the 'false positive' background for each species of dimer in each experiment and subtract it from the total number counted. The uncertainty in this background correction is $(N_{FP})^{1/2}$.

Curve fitting

Relative uncertainties in data were estimated as follows (see above):

$$\frac{\delta[A{:}B]}{[A{:}B]} = \left(\frac{1}{N_{AB}} + \frac{N_{FP}}{N_{AB}^2} + \delta c\right)^{\frac{1}{2}} \text{ etc.}$$

$$\frac{\delta([A]\times[B])}{[A]\times[B]} = \left(\frac{1}{N_A} + \frac{1}{N_B} + 2\delta c\right)^{\frac{1}{2}}$$

$$\frac{\delta([A]^2)}{[A]^2} = 2\left(\frac{1}{N_A} + \delta c\right)^{\frac{1}{2}} \text{ etc.}$$

Uncertainties (Err) in data used as input parameters for the linear fits used to estimate K_ds are listed in Table S5.

Assessments of fits, errors

Linear fits to graphs of $[A_n] \times [B_n]$ vs. $[A_n{:}B_n]$ etc. were obtained using OriginPro, with uncertainties in both quantities calculated as described above and listed in Table S5. The gradient of the fitted line was accepted as a useful measure of K_d if the change in fitted gradient on constraining the line to pass through the origin was <30%. Errors quoted in Table 1 are standard errors on the gradient of the constrained fits and do not include systematic errors discussed above.

Supporting Figures

a: CC-Di-EN4

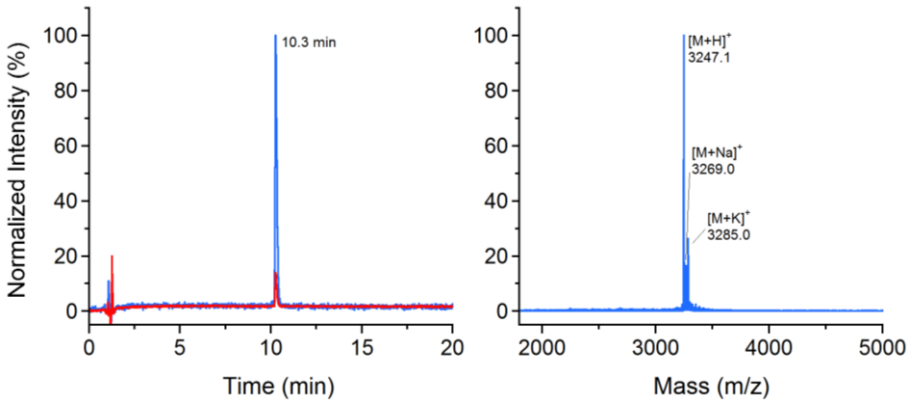

Sequence: Ac-G EIAALEQ EIAALEQ KNAALKW KIAALKQ G-NH_2
Gradient: 20–60% Buffer B. $[M+H]^+$ expected mass = 3246.8 Da, observed mass = 3247.1 Da.

b: CC-Di-KN4

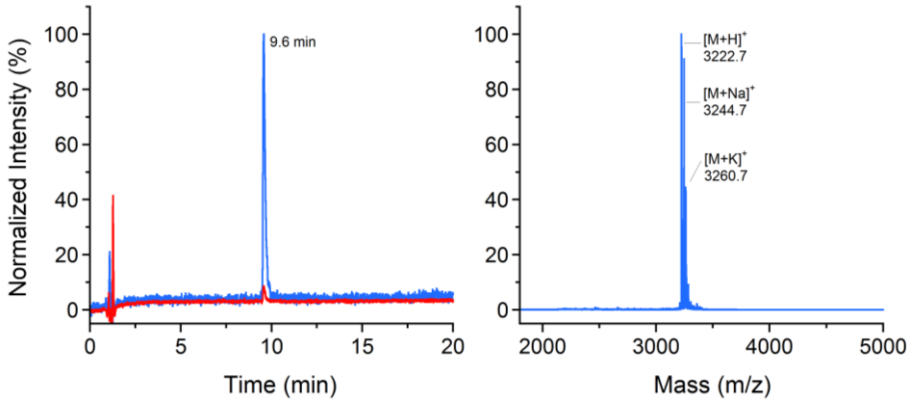

Sequence: Ac-G KIAALKQ KIAALKY ENAALEQ EIAALEQ G-NH_2
Gradient: 20–60% Buffer B, $[M+H]^+$ expected mass = 3223.8 Da, observed mass = 3222.7 Da.

c: CC-Di-EN3.5

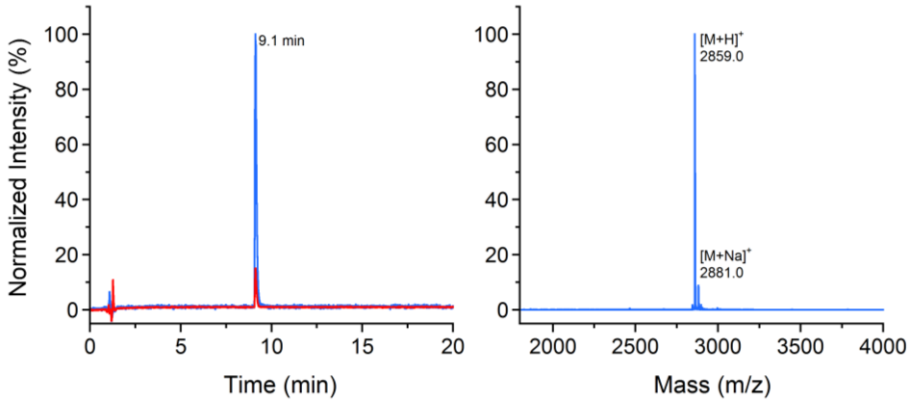

Sequence: Ac-G LEQ EIAALEQ KNAALKW KIAALKQ G-NH_2
Gradient: 20–60% Buffer B. $[M+H]^+$ expected mass = 2861.6 Da, observed mass = 2859.0 Da.

d: CC-Di-KN3.5

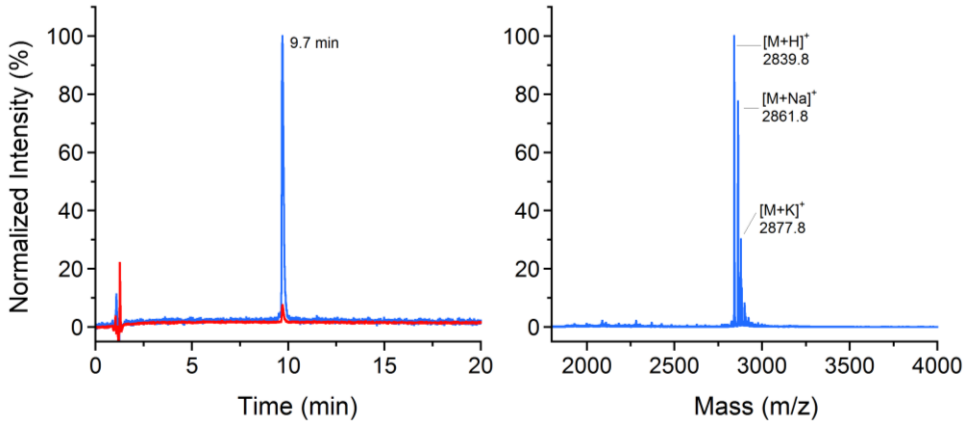

Sequence: Ac-G LKQ KIAALKY ENAALEQ EIAALEQ G-NH_2
Gradient: 20–60% Buffer B. $[M+H]^+$ expected mass = 2840.5 Da, observed mass = 2839.8 Da.

e: CC-Di-EN3

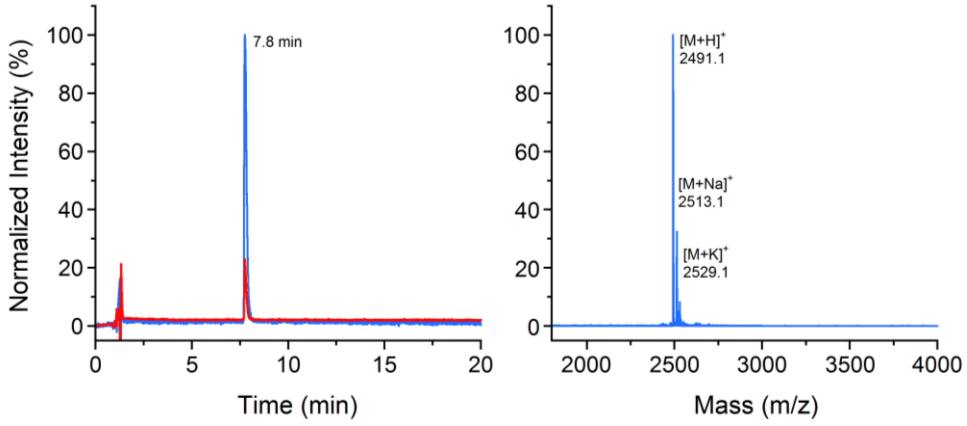

Sequence: Ac-G EIAALEQ KNAALKW KIAALKQ G-NH_2
Gradient: 20–60% Buffer B. $[M+H]^+$ expected mass: 2492.4 Da, observed mass = 2491.1 Da.

f: CC-Di-KN3

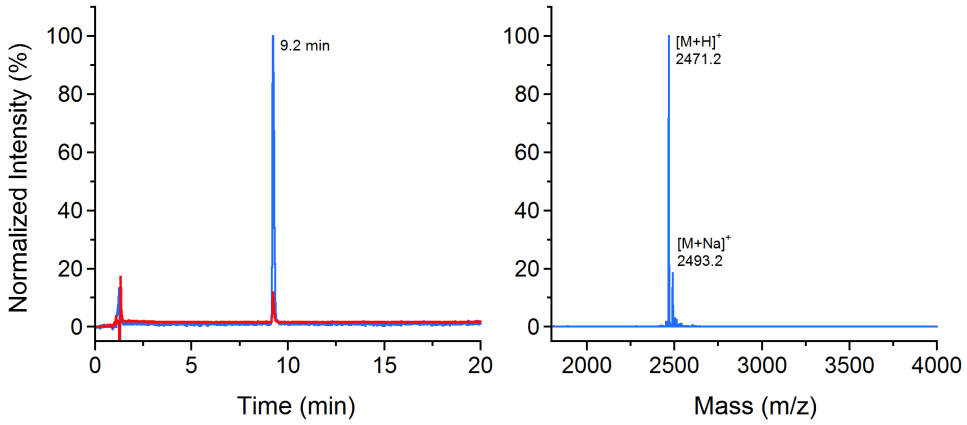

Sequence: Ac-G KIAALKY ENAALEQ EIAALEQ G-NH_2
Gradient: 20–60% Buffer B. $[M+H]^+$ expected mass = 2471.3 Da, observed mass = 2471.2 Da.

g: CC-Di-EK

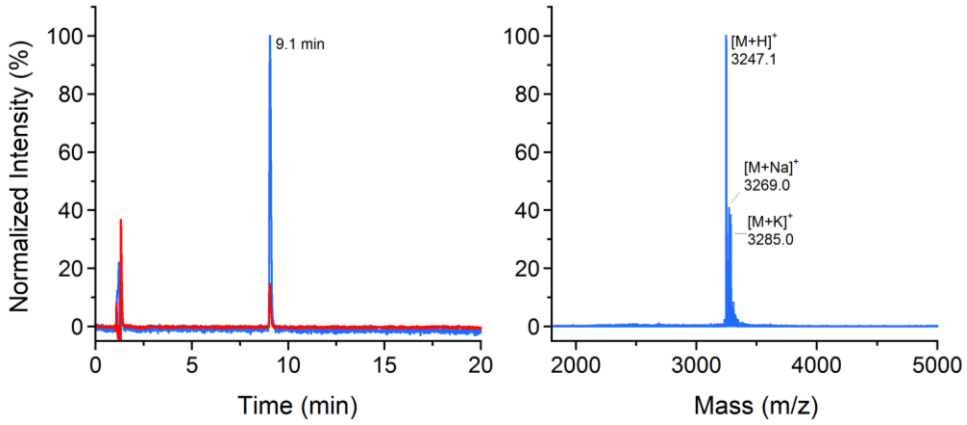

Sequence: Ac-G EIAALEQ ENAALEQ KIAALKW KNAALKQ G-NH_2
Gradient: 20–60% Buffer B. $[M+H]^+$ expected mass = 3246.8 Da, observed mass = 3247.1 Da.

h: CC-Di-KE

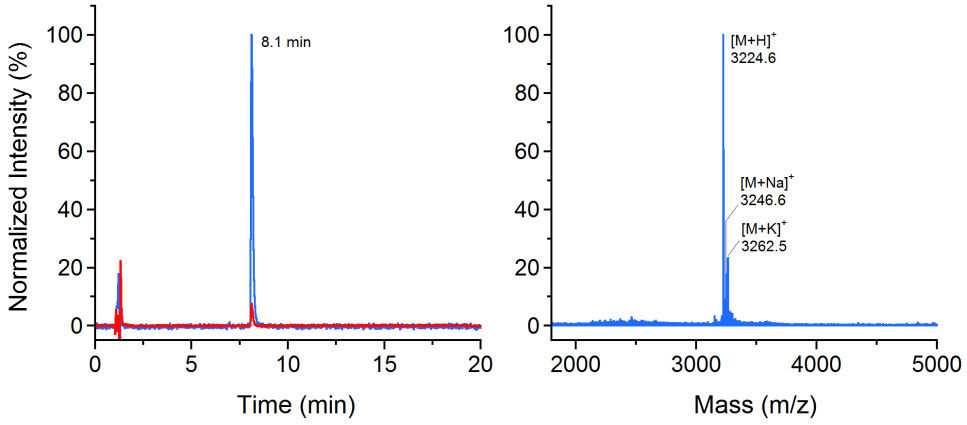

Sequence: Ac-G KIAALKQ KNAALKY EIAALEQ ENAALEQ G-NH_2
Gradient: 20 - 60% Buffer B. $[M+H]^+$ expected mass = 3224.7 Da, observed mass = 3224.6 Da.

i: CC-Di-EK-Z

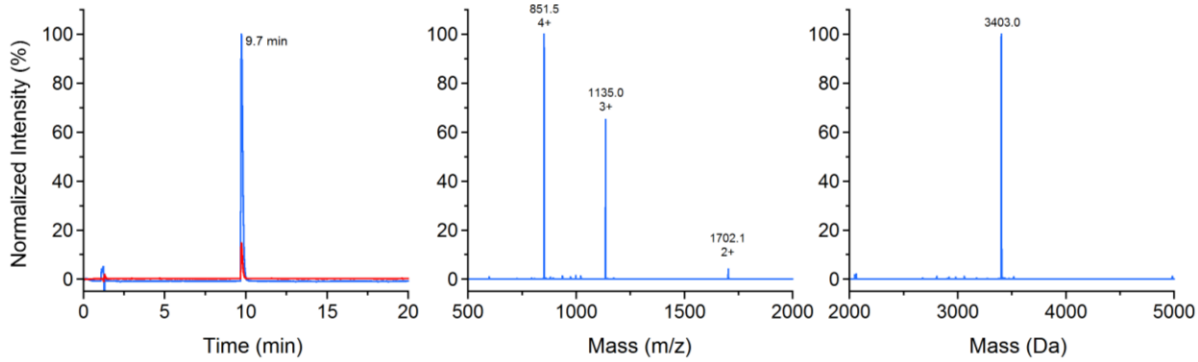

Sequence: Ac-G EIAALEQ ENAALEQ KIAALKW KNAALKQ GZ-NH_2 z=azidonorleucine
Gradient: 20–60% Buffer B. $[M+H]^+$ expected mass = 3402.9 Da, observed mass = 3403.0 Da.

j: Z-CC-Di-KE

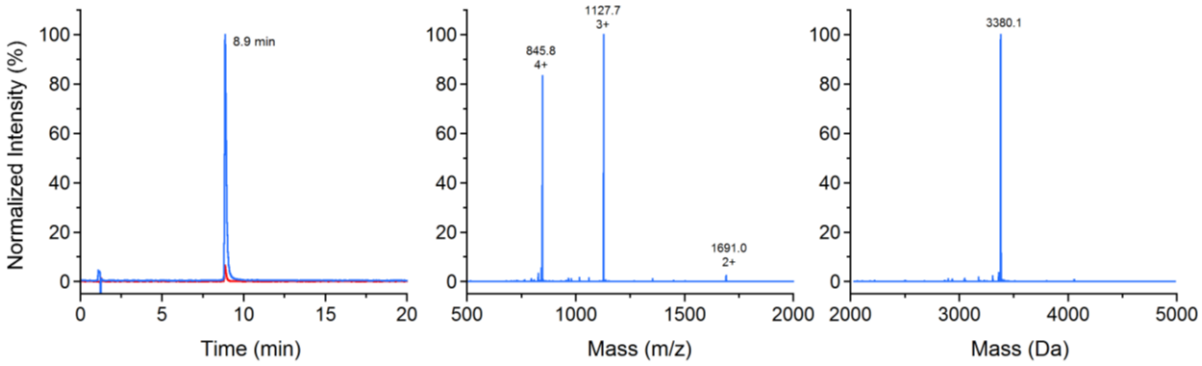

Sequence: Ac-ZG KIAALKQ KNAALKY EIAALEQ ENAALEQ G-NH_2 z=azidonorleucine
Gradient: 20–60% Buffer B. $[M+H]^+$ expected mass = 3379.8 Da, observed mass = 3380.1 Da.

k: C-CC-Di-EK

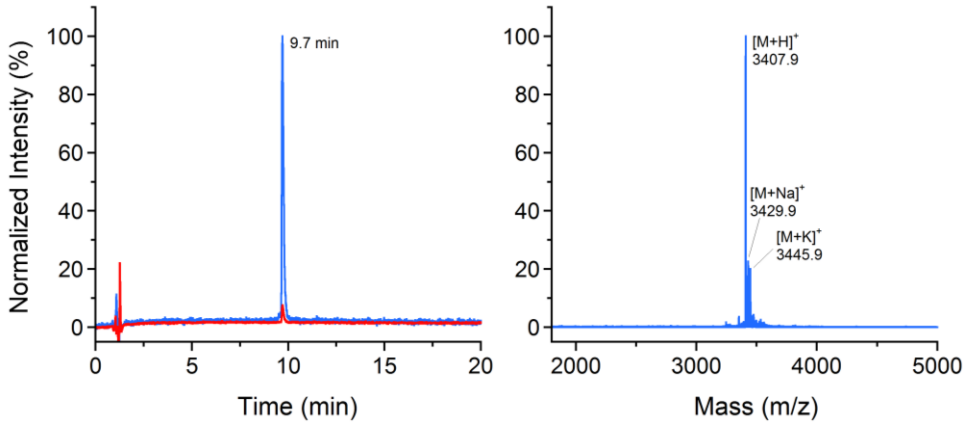

Sequence: Ac-CGG EIAALEQ ENAALEQ KIAALKW KNAALKQ G-NH_2
Gradient: 20–70% Buffer B. $[M+H]^+$ expected mass = 3407.8 Da, observed mass = 3407.9 Da.

l: CC-Di-EK-C

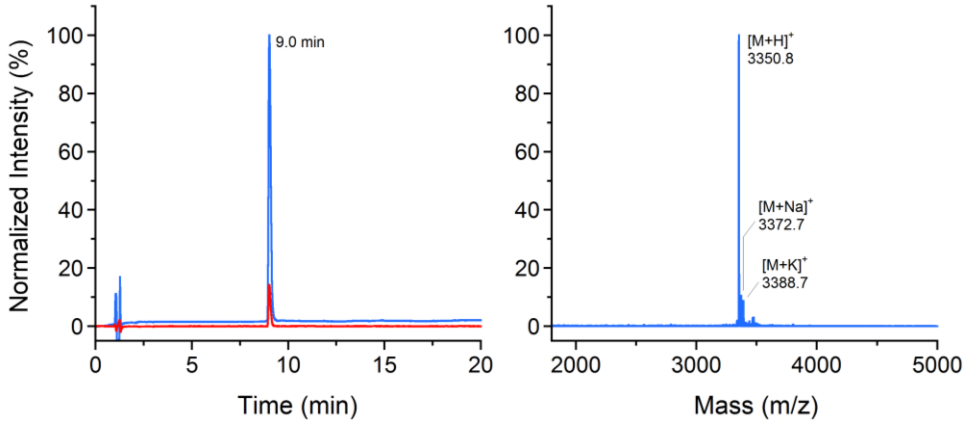

Sequence: Ac-G EIAALEQ ENAALEQ KIAALKW KNAALKQ GC-NH_2
Gradient: 20–70% Buffer B. $[M+H]^+$ expected mass = 3350.8 Da, observed mass = 3350.8 Da.

m: C-CC-Di-KE

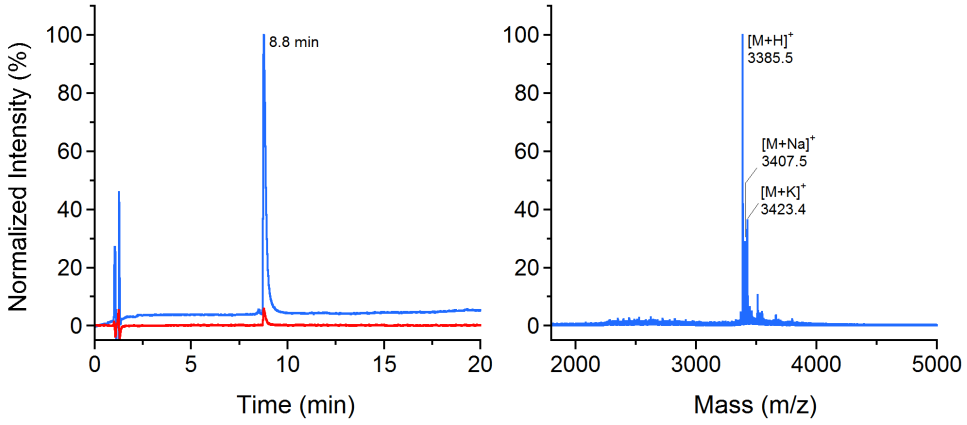

Sequence: Ac-CGG KIAALKQ KNAALKY EIAALEQ ENAALEQ G-NH_2
Gradient: 20–70% Buffer B. $[M+H]^+$ expected mass = 3386.9 Da, observed mass = 3385.5 Da.

n: CC-Di-KE-C

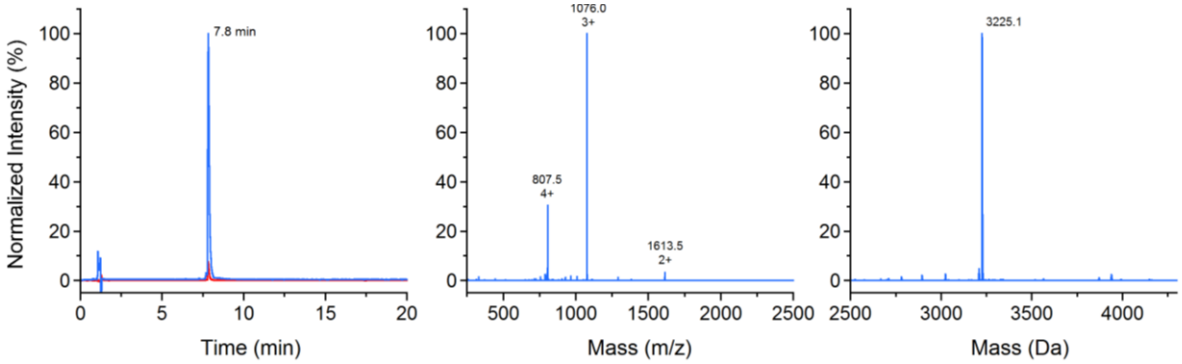

Sequence: Ac-G KIAALKQ KNAALKY EIAALEQ ENAALEQ GC-NH_2
Gradient: 20 - 70% Buffer B. $[M+H]^+$ expected mass = 3326.8 Da, observed mass = 3225.1 Da.

o: CC-Di-EK-C
|
CC-Di-KE-C

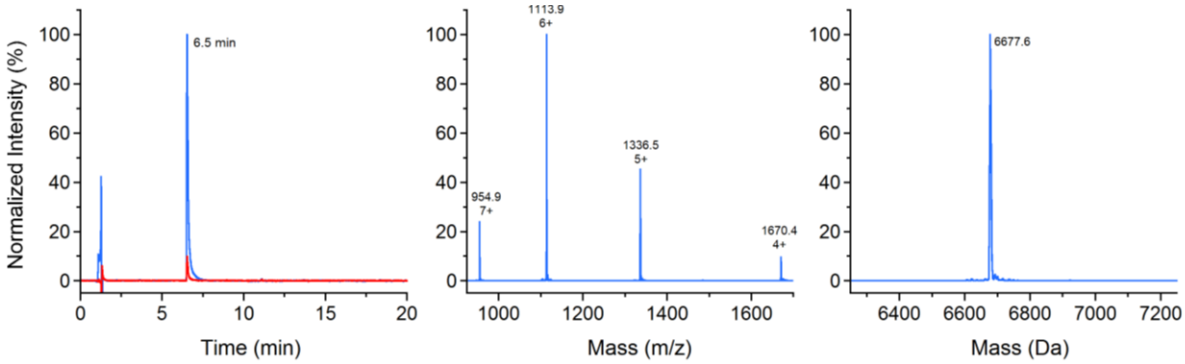

Sequence:
Ac-G EIAALEQ ENAALEQ KIAALKW KNAALKQ GC-NH_2
|
Ac-G KIAALKQ KNAALKY EIAALEQ ENAALEQ GC-NH_2
Gradient: 20–70% Buffer B. Expected mass = 6678.7 Da, observed mass = 6677.6 Da.

p: CC-Di-EK-C
|
C-CC-Di-KE

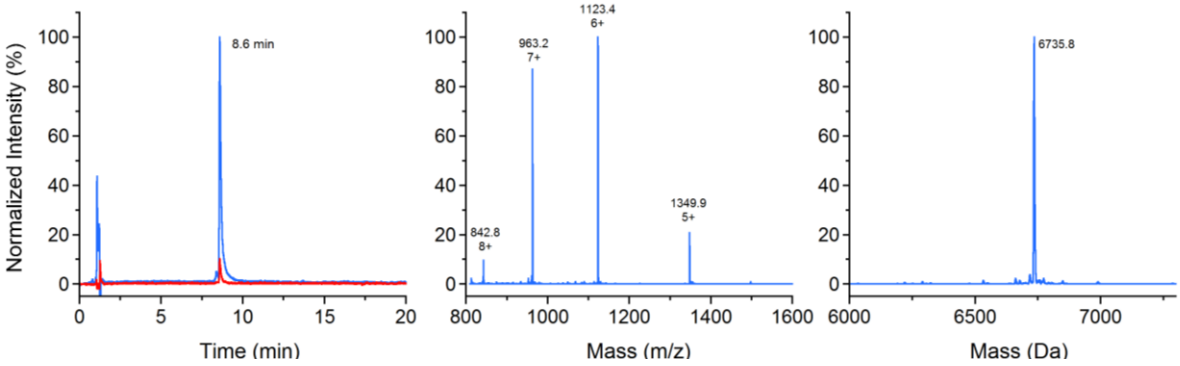

Sequence:
Ac-G EIAALEQ ENAALEQ KIAALKW KNAALKQ GC-NH_2
|
Ac-CGG KIAALKQ KNAALKY EIAALEQ ENAALEQ G-NH_2

Gradient: 20–70 % Buffer B. Expected mass = 6735.7 Da, observed mass = 6735.8 Da.

Figure S1 Mass spectrometry and analytical HPLC characterization of peptides. (**a**-**p**) Left: Analytical HPLC traces showing >98% peptide purities, (**a**-**h**, **k**-**m**) Right: MALDI-TOF mass spectra. (**i**, **j**, **n**-**p**), Middle: Nanospray-TOF mass spectra and Right: deconvoluted mass spectra.

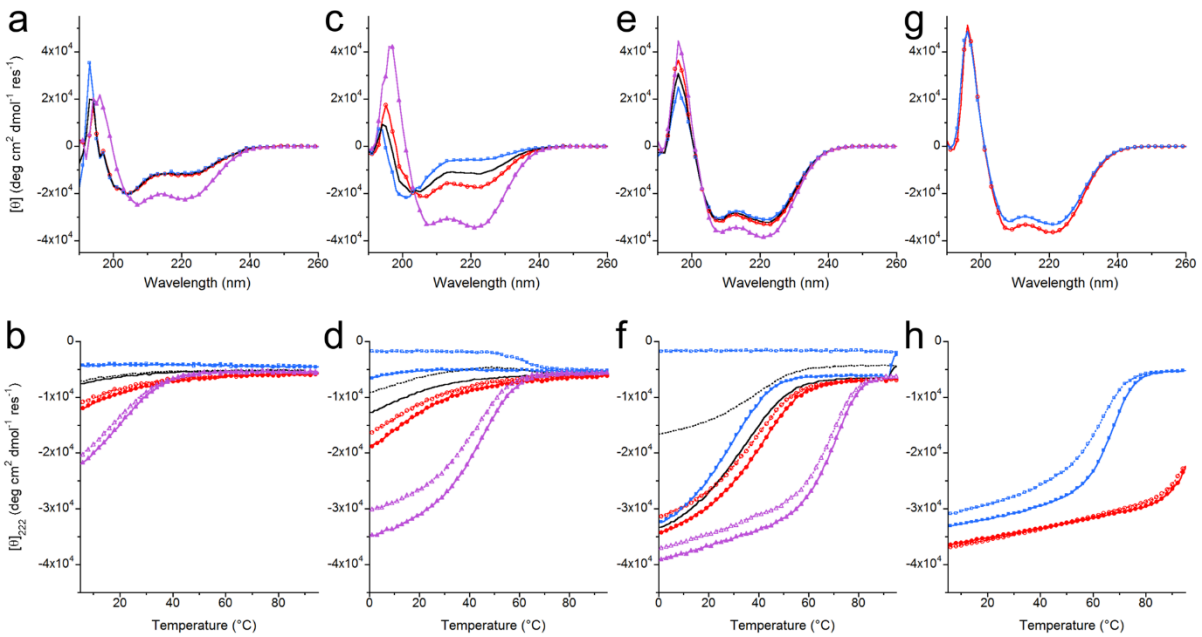

Figure S2 Additional CD spectra and thermal unfolding transitions for peptides. CD spectra recorded at 5°C, (**a**, **c**, **e** and **g**) and thermal unfolding transitions (**b**, **d**, **f** and **h**) monitored through the CD signal at 222 nm. Conditions: 50 μM of each peptide in PBS buffer (pH 7.4).
Samples:
(**a**&**b**) CC-Di-EN3 (red, circles), CC-Di-KN3 (blue, squares) and CC-Di-EN3:KN3 (purple, triangles);
(**c**&**d**) CC-Di-EN3.5 (red, circles), CC-Di-KN3.5 (blue, squares) and CC-Di-EN3.5:KN3.5 (purple, triangles);
(**e**&**f**) CC-Di-EN4 (red, circles), CC-Di-KN4 (blue, squares) and CC-Di-EN4:KN4 (purple, triangles);
(**g**&**h**) CC-Di-EK-C | CC-Di-KE-C (red, circles) and CC-Di-EK-C | C-CC-Di-KE (blue, squares).

Averages of the CD spectra and thermal unfolding profiles for the individual peptides are shown in black. Thermal unfolding and refolding profiles are shown by filled and open symbols with solid and dashed lines, respectively. Midpoints of thermal unfolding transitions were estimated, where possible, from the positions of maxima of the first derivatives and are given in Table S2.

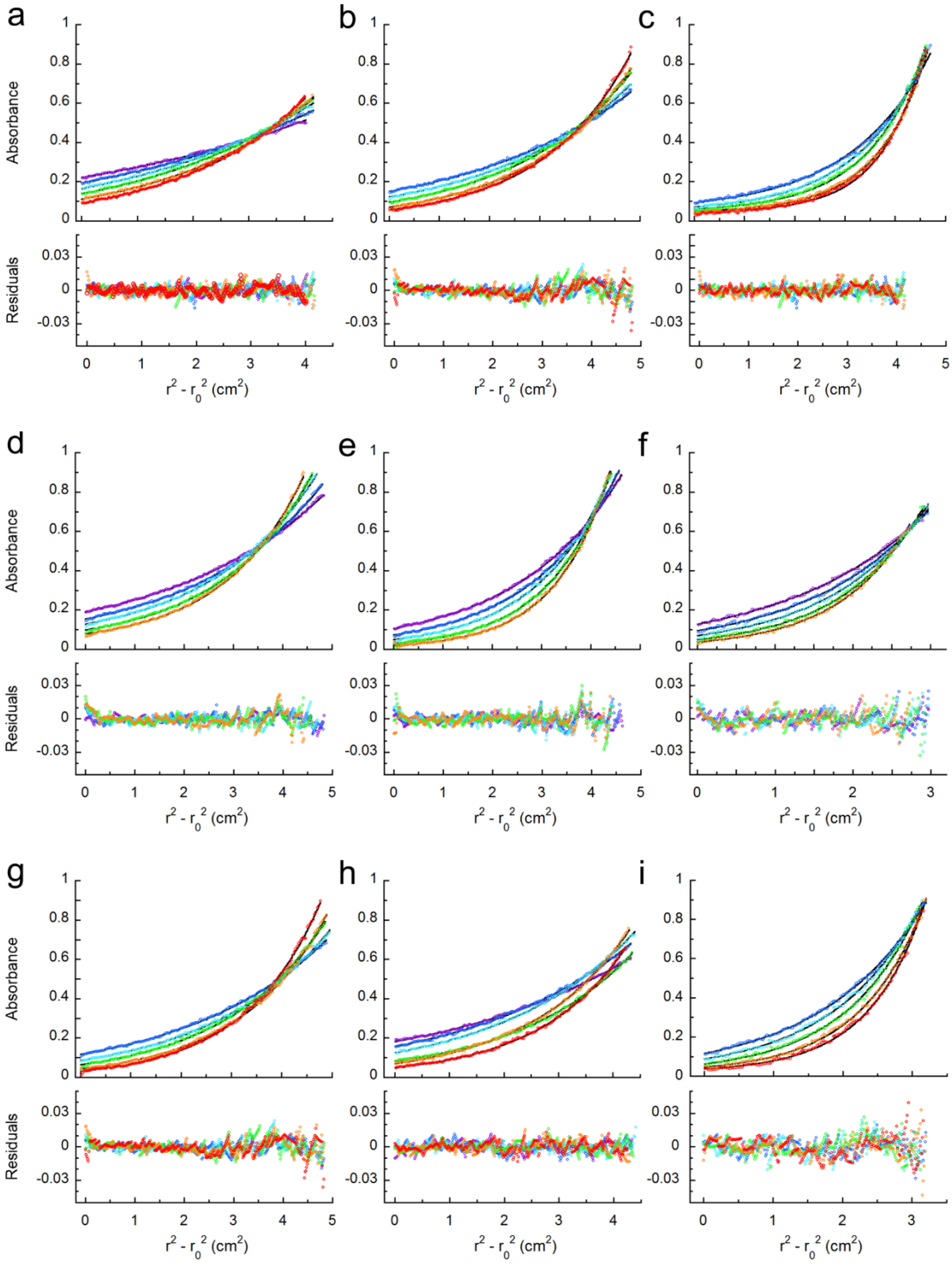
a
b
c
d
e
f
g
h
i
Absorbance
Residuals
r² - r₀² (cm²)

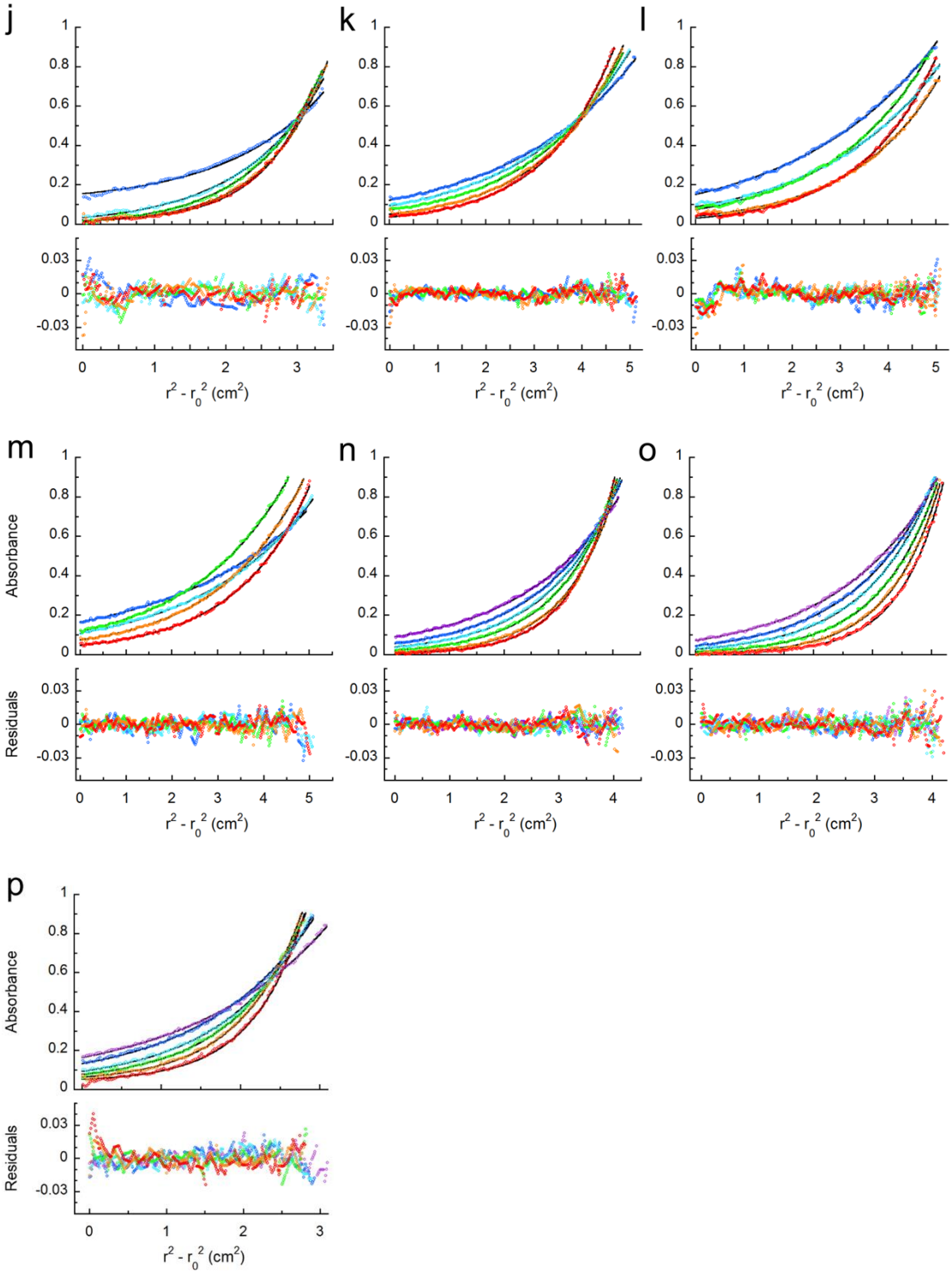

Figure S3 Additional AUC data for peptides. Sedimentation equilibrium AUC data (top, circles) and fits to single ideal species models (top, black lines) with residuals for the fits (circles, bottom) plotted against $r^2 - r_0^2$ (r, radius of the sample from the centre of the rotor and a reference radius, r_0. The masses returned from the fits are given in Table S3. **Colour Key (a–n):** 40 krpm (purple), 44 krpm (blue), 48 krpm (cyan), 52 krpm (green), 56 krpm (orange), 60 krpm (red). **Colour Key (o, p):** 24 krpm (purple), 27 krpm (blue), 30 krpm (cyan), 33 krpm (green), 36 krpm (orange), 39 krpm (red).

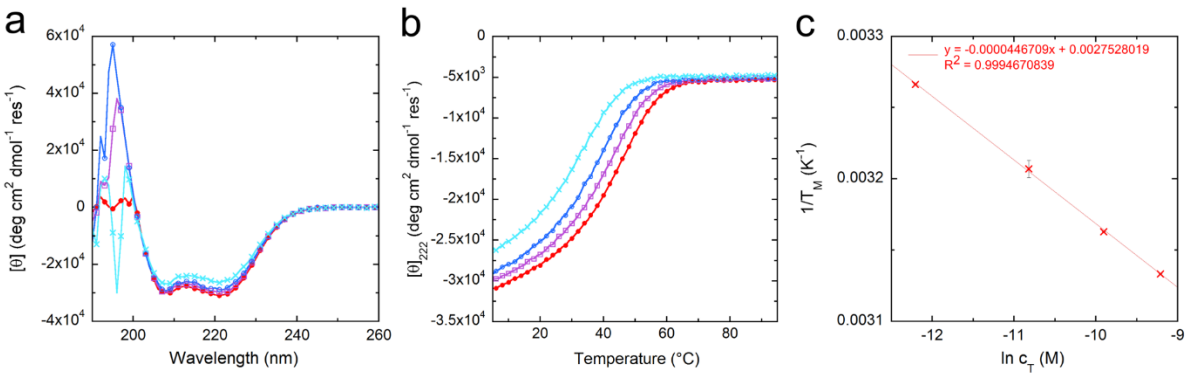

Figure S4 Determination of K_d for CC-Di-EK:KE dimer by CD spectroscopy. (**a**) Representative CD spectra recorded at 5°C. (**b**) Representative thermal unfolding profiles recorded at 222 nm. (**c**) K_d analyses of the CD data following the method of Marky and Breslauer for non-self-complementary sequences.[2] The K_d was determined from the slope of a linear plot of the recorded T_M (an average of three measurements) vs. total peptide concentration to be 102±26 μM. **Key** (**a**&**b**)**:** 100 μM (red, filled circles), 50 μM (lilac, squares), 20 μM (blue, squares), 5 μM (cyan, saltires) of each peptide component, CC-Di-EK and CC-Di-KE. Experiments were performed in PBS buffer (pH 7.4).

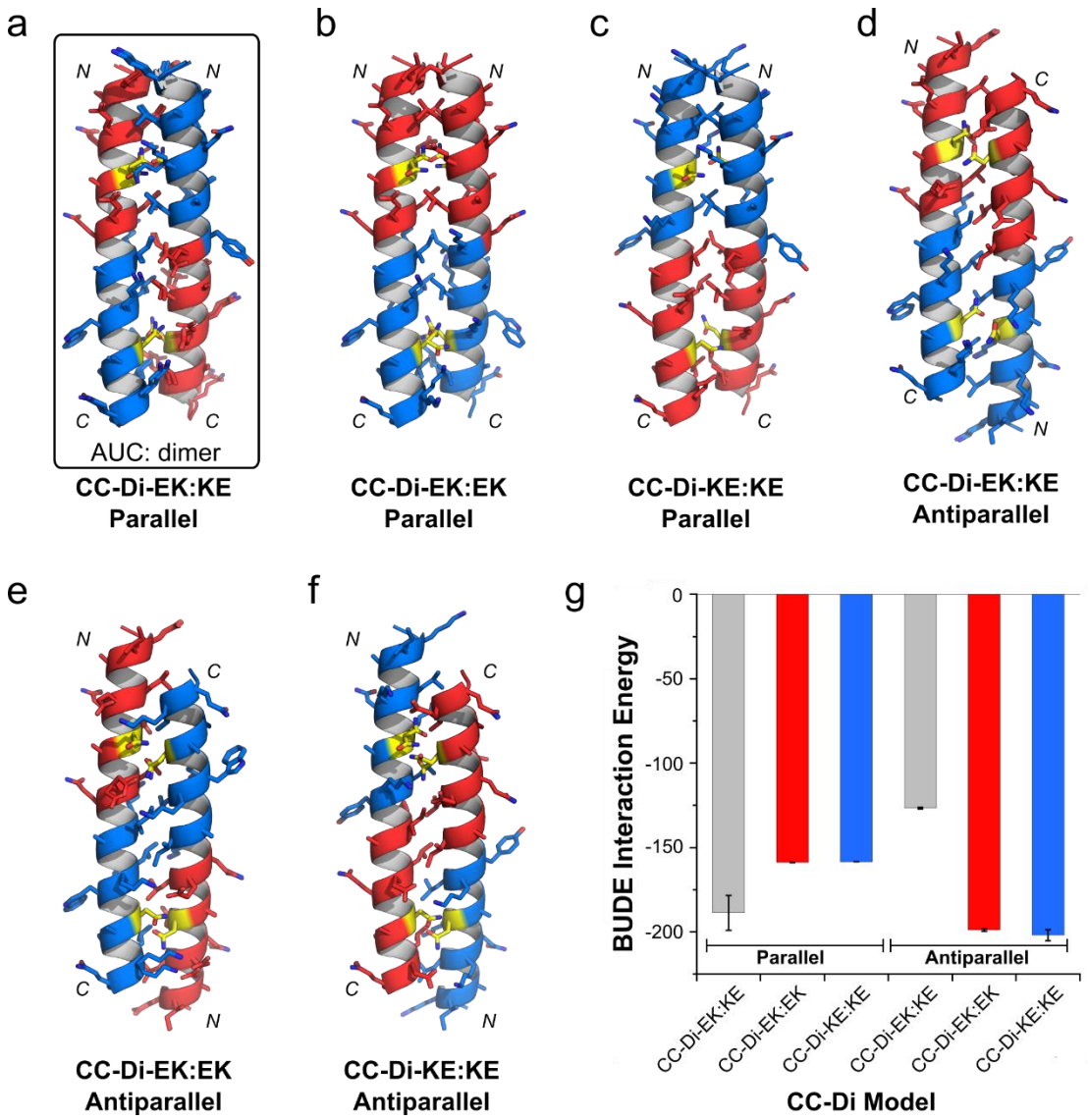

Figure S5 Heterodimer models. Models for the six hypothetical combinations of CC-Di-EK and CC-Di-KE as forced parallel and antiparallel hetero- and homodimers were generated and optimized in ISAMBARD,[1] using geometric parameters suitable for coiled-coil dimers (see Supporting Methods). (**a**–**f**) Overlays of the lowest-energy models from three separate runs for each theoretical coiled coil dimer show good convergence. Please note that only CC-Di-EK:KE is dimeric in solution (boxed) and models B, C, D and E, *i.e.* homodimers, do not exist at the concentrations studied. (**g**) BUDE interaction energies for the models in a–f. CC-Di-EK:KE is most stable in the parallel arrangement as designed (a vs. d), due to favourable placements of charged side chains at core-flanking 'e' and 'g' sites, in addition to dimer-specifying and stabilizing asparagine at 'a'-sites within the core (yellow). The antiparallel heterodimer is disfavoured (d&g – gray bars). The forced antiparallel dimers adopt slipped conformations to maintain Asn at 'a' pairs and minimize disruption to the hydrophobic cores. Interestingly, though not surprising, the hypothetical antiparallel homodimers CC-Di-EK:EK and CC-Di-KE:KE score well (e, f, & g); this is likely due to an artefact of the BUDE force field which overweighs interhelical salt bridge pairs, of which there are many in these models.

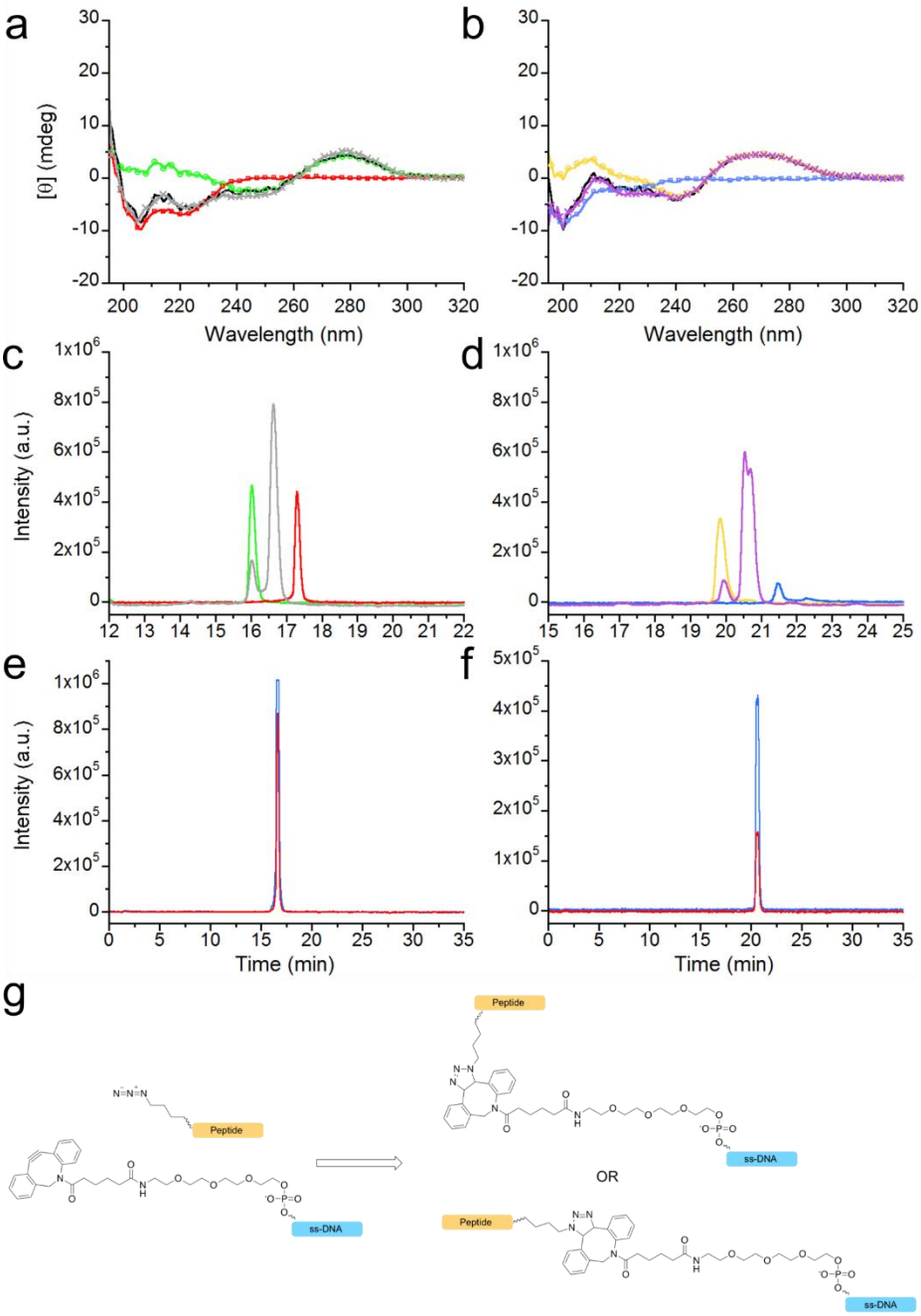

Figure S6 Peptide-DNA conjugation. (**a**&**b**) CD spectra of parent peptides, oligo-tags and 1:1 mixtures of the two at 15 μM of each component in PBS (pH 7.4) show no interaction. (**a**) CC-Di-EK peptide (red, squares), oligo-tag-α (green, circles), 1:1 CC-Di-EK and oligo-tag-α (gray, saltires), and the expected spectrum of the mixture assuming no interaction (black, line). (**b**) CC-Di-KE peptide (blue, squares), oligo-tag-β (mustard, circles) 1:1 CC-Di-KE and oligo-tag-β (purple, saltires), and the expected spectrum of the mixture (black, line). (**c&d**) Conjugation reactions, monitored by analytical HPLC at 280 nm, between azide functionalised peptides CC-Di-EK-Z (red) and Z-CC-Di-KE (blue) with oligo tags α (green) and β (mustard) respectively, for formation of CC-Di-EK-α (gray) (**c**) and β-CC-Di-KE (purple) (**d**). (**e**&**f**) Analytical HPLC traces for the purified peptide-oligonucleotide conjugates, CC-Di-EK-α (**e**) and β-CC-Di-KE (**f**) monitored at 280 nm (red) and 260 nm (blue). (**g**) Reaction scheme for copper-free 1-3 Huisgen cycloaddition of azide-functionalzed peptide to dibenzylcyclooctyne-functionalized oligo tags.

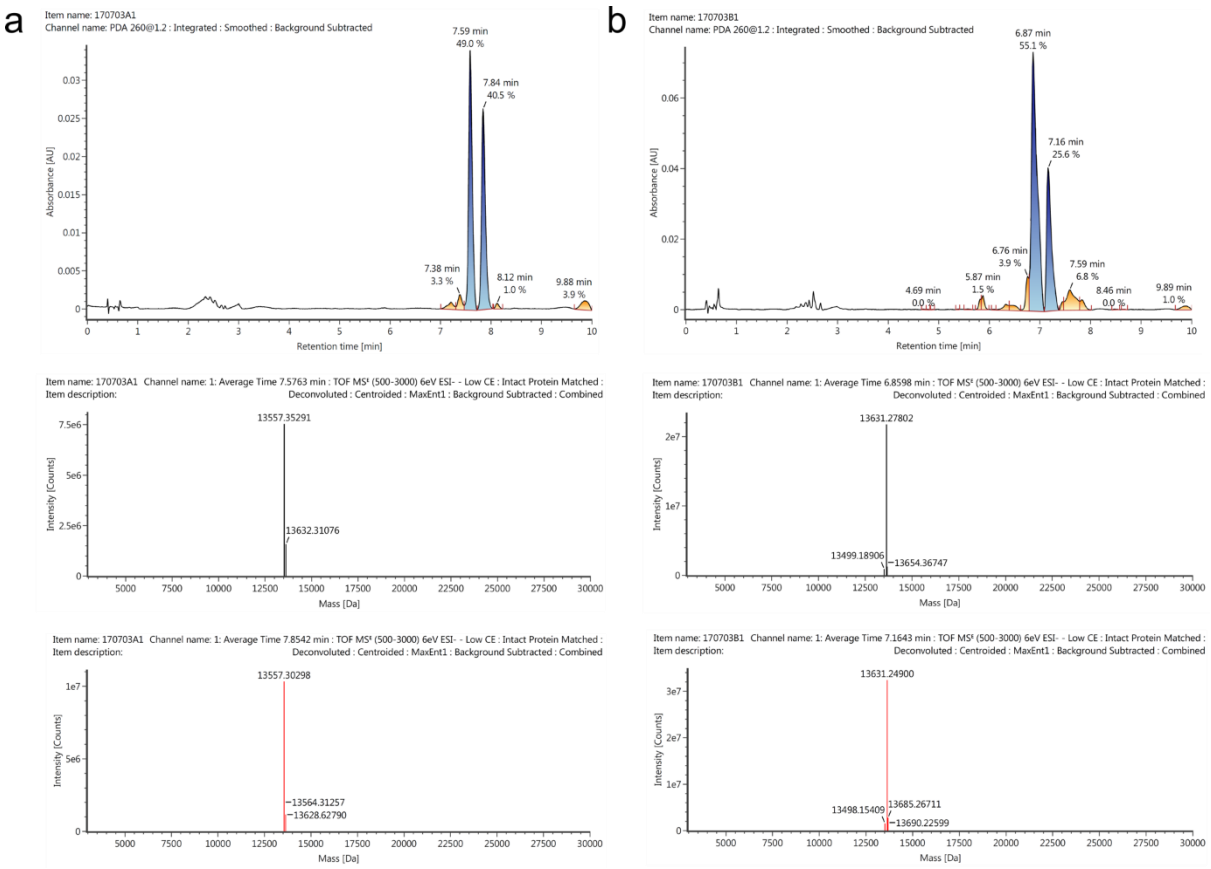

Figure S7 LC-MS data for peptide-oligonucleotide conjugates. (**a**) CC-Di-EK-α, (**b**) β-CC-Di-KE. Top: LC chromatograms in which the two regioisomers of each conjugate are resolved (see Figure S6g). Middle and bottom: deconvoluted mass spectra of conjugate peaks (blue, top). CC-Di-EK-α expected mass = 13557 Da (observed mass = 13557 Da), β-CC-Di-KE expected mass = 13631 Da (observed mass = 13631 Da).

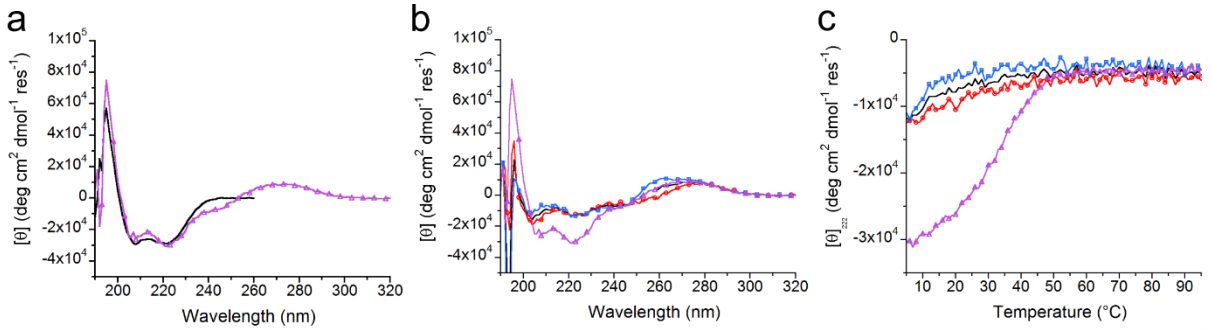

Figure S8 CD spectra of peptide-oligonucleotide conjugates. (**a**&**b**) CD spectra recorded at 5°C of (**a**) parent peptide dimer, CC-Di-EK:KE at 10 μM of each peptide (black) vs. 1:1 mixture of DNA functionalized peptides CC-Di-EK-α and β-CC-Di-KE at 10 μM each (purple, triangles) and (**b**) CC-Di-EK-α (red, circles), β-CC-Di-KE (blue, squares), the average spectrum of the oligo-tagged peptides (black) and 1:1 mixture of CC-Di-EK-α : β-CC-Di-KE (purple, triangles). (**c**) Thermal unfolding profiles of the peptide conjugates monitored at 222 nm. Color Key as in part b. In parts b&c oligo-tagged peptides are 10 μM each.

a

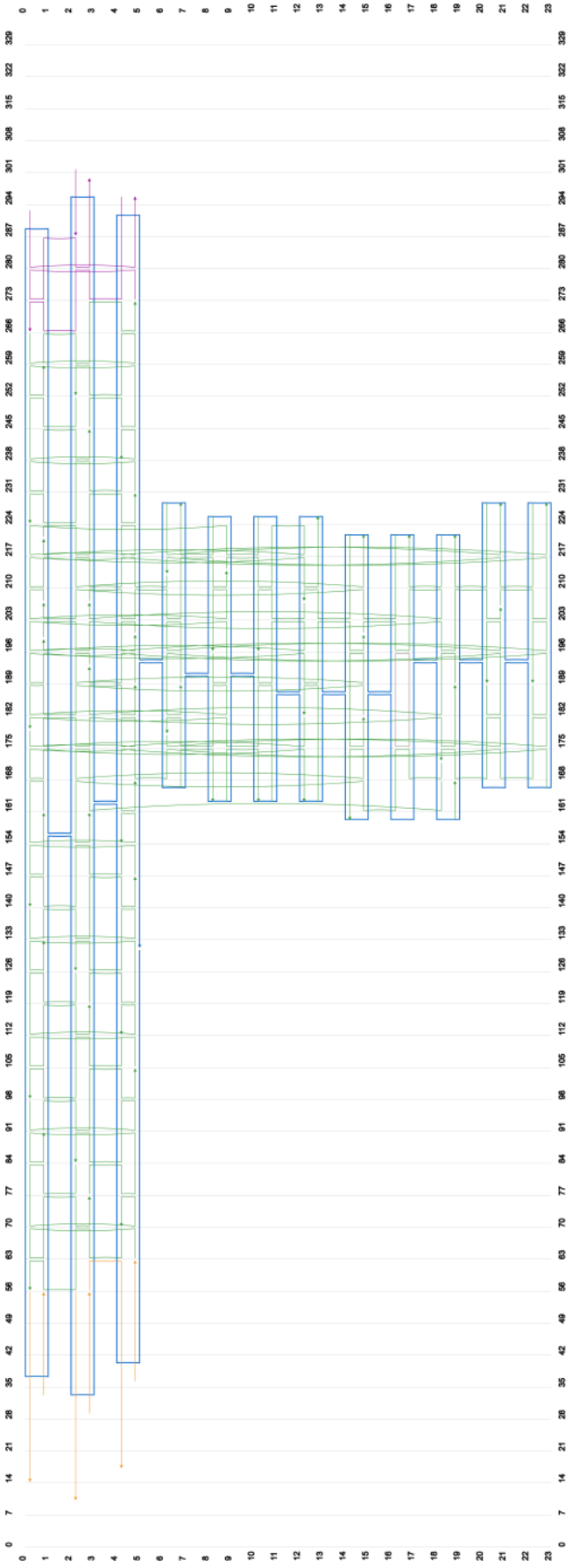

b

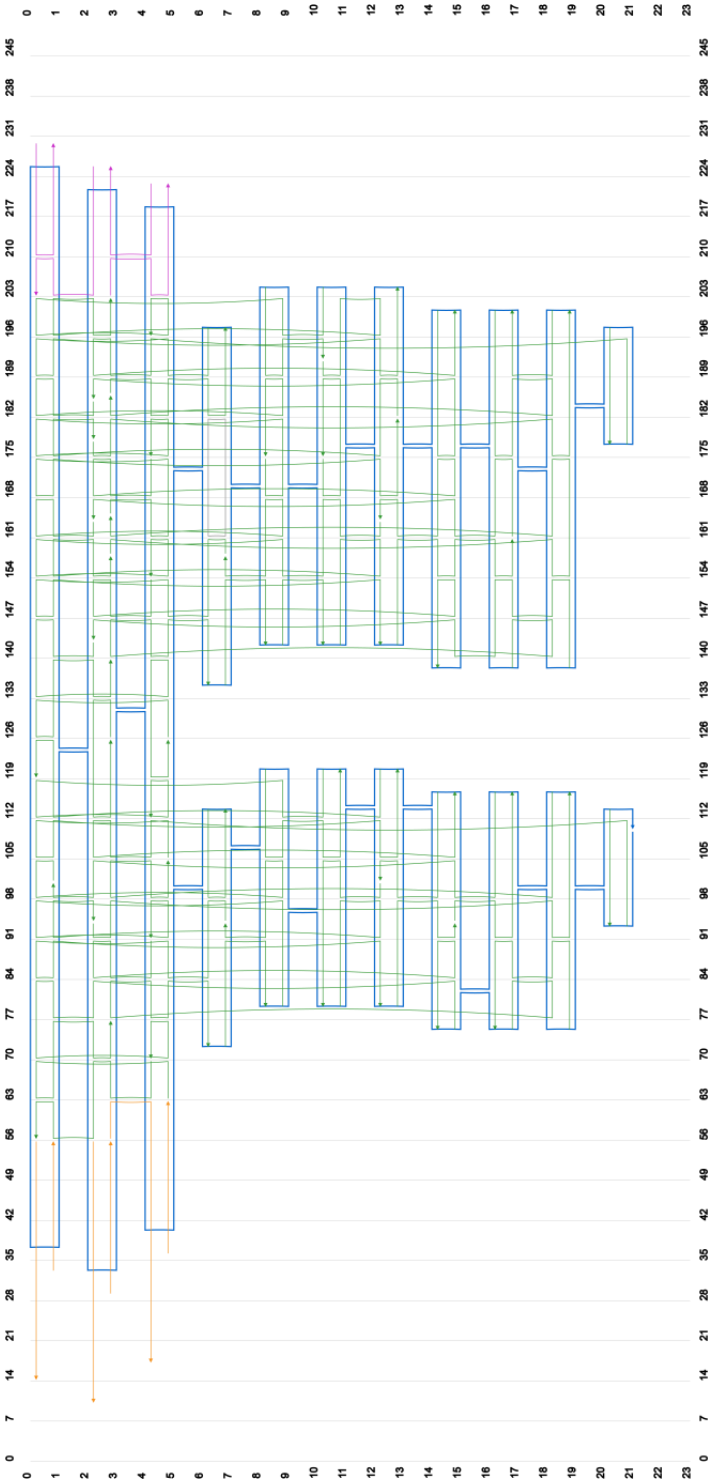

Figure S9 CaDNAno[5] diagrams of DNA origami staple layouts. (**a**) Origami A; (**b**) Origami B. The scaffold strands are marked in blue. Staple strands are divided into three groups: left end (at the bottom in this diagram) containing handle strands (orange); middle part containing DNA sleeves (green); and the unfunctionalized right end (magenta). Single-stranded extensions to staple strands at the left ends of helices 0, 2, and 4 are handle sequences (+23 nt). There are shorter single-stranded polythymidine extensions to staple strands at the left ends of helices 1, 3 and 5 and the right ends of helices 0, 1, 2, 3, 4 and 5 (T_4 in all cases but the right hand end of helix 2 of origami A, which is extended by T_6).

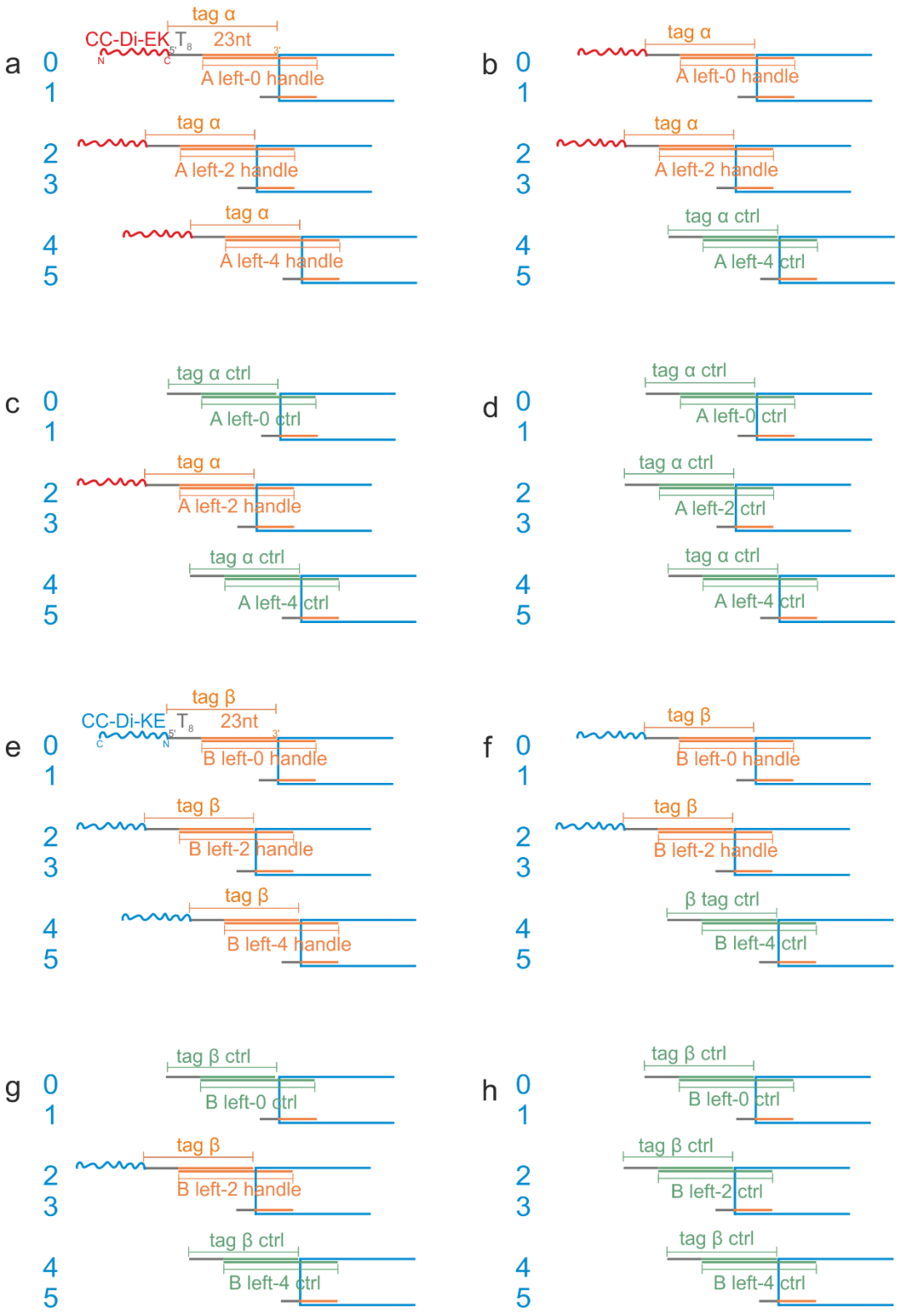

Figure S10 Diagrams of the ends of DNA origamis decorated with different numbers of peptides. Origami A is decorated with different numbers of CC-Di-EK-α: (**a**) A_3, (**b**) A_2 (**c**) A_1 and (**d**) A_0. Origami B is decorated with different numbers of CC-Di-KE-β: (**e**) B_3, (**f**) B_2, (**g**) B_1 and (**h**) B_0. The DNA helices from which the handles protrude do not finish flush (see Figure S9).

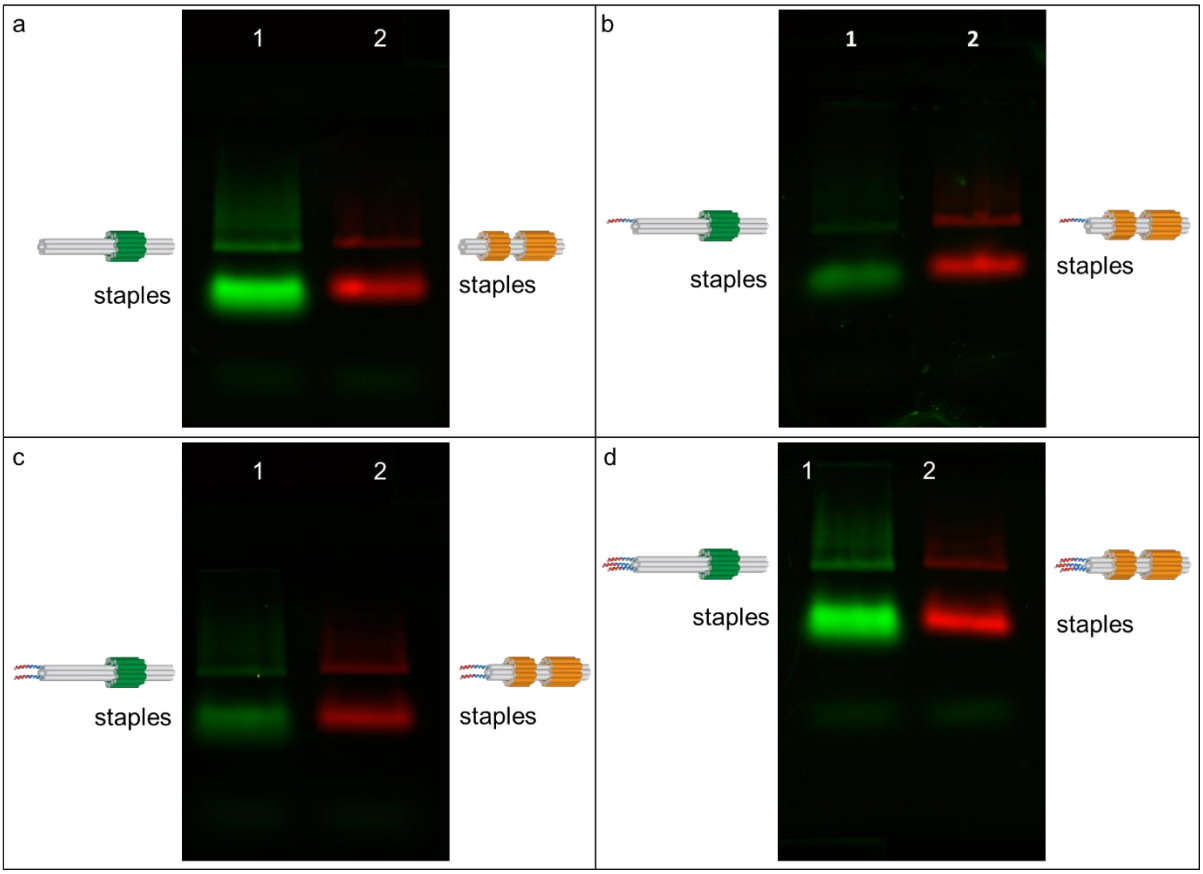

Figure S11-1 Gel electrophoresis of DNA origamis and DNA origamis decorated with peptides. (**a**) A_0 and B_0, (**b**) A_1 and B_1; (**c**) A_2 and B_2; (**d**) A_3 and B_3. One staple strand in Origami A is labelled with fluorophore Cy3 (green; for details see Table S6-1) and one staple strand in Origami B is labelled with Cy5 (red; for details see Table S6-2). Conditions: 0.8% (w/v) agarose gel run in 0.5×TBE buffer with 11 mM $MgCl_2$ in an ice bath, 60V for 180 min (a),170 min (b), 158 min (c) and 138min (d).

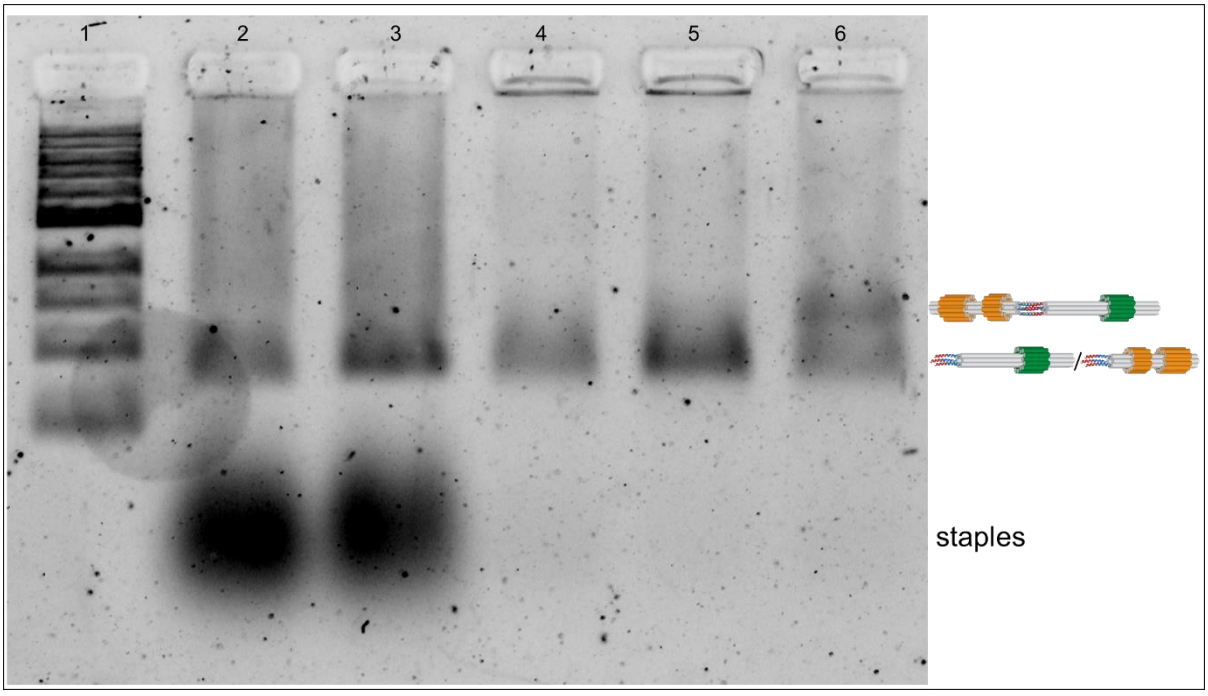

Figure S11-2 Gel electrophoresis of peptide-mediated origami assembly (n=3). Lane 1: 1kb DNA ladder; 2: mixture of Origami A with CC-Di-EK-α; 3: mixture of origami B with β-CC-Di-KE; 4: purified A_3; 5: purified B_3; 6: mixture of purified A_3 and B_3. Conditions: 1.5% (w/v) agarose gel, sample run in 0.5×TBE buffer with 11 mM $MgCl_2$ in an ice bath, 60V for 150min. Gel was post-stained with 1×Sybr® Gold (Thermo Fisher Scientific).

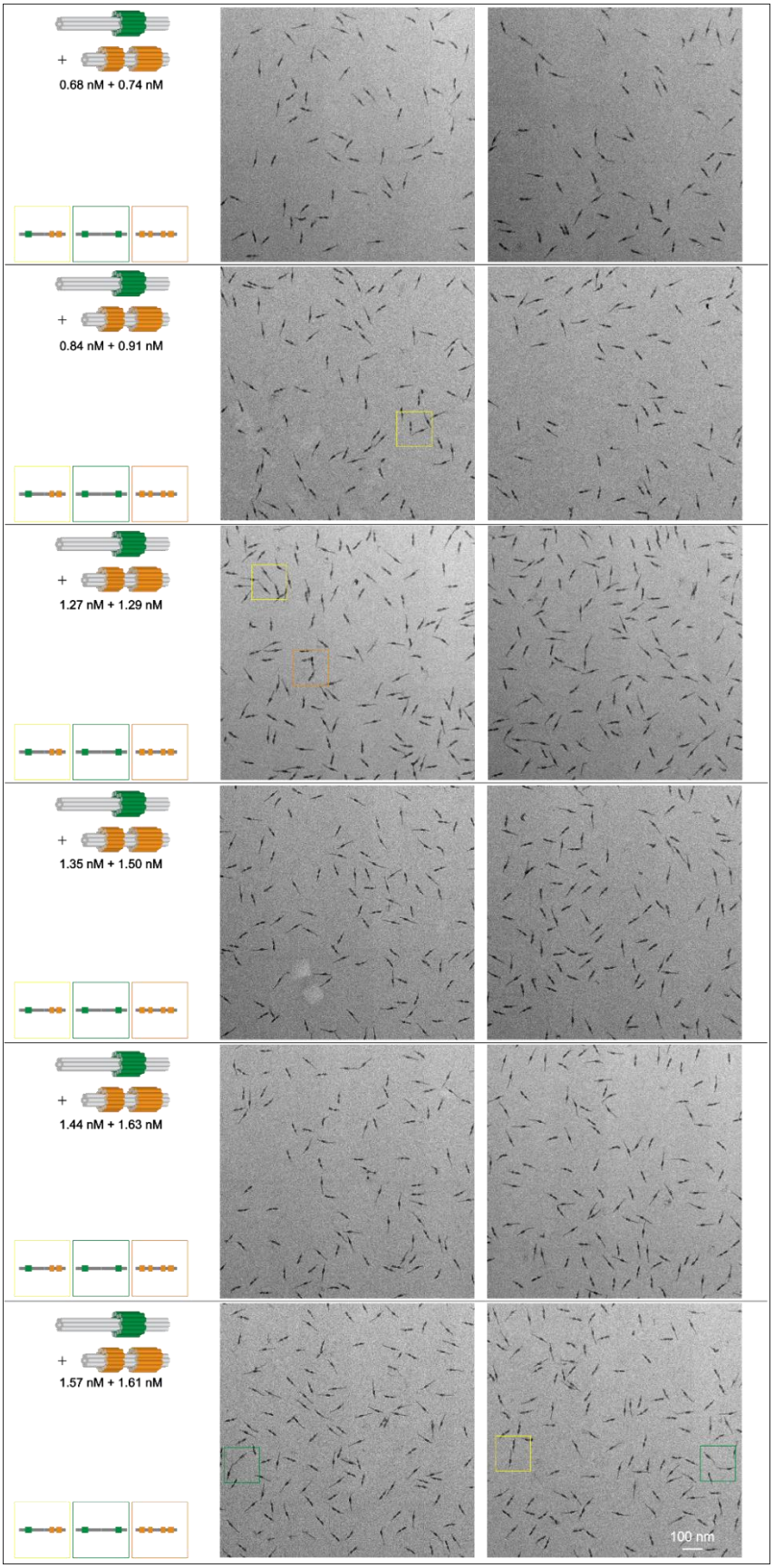

Figure S12-1 Representative TEM images of mixture of A_0 and B_0 at different initial concentrations.

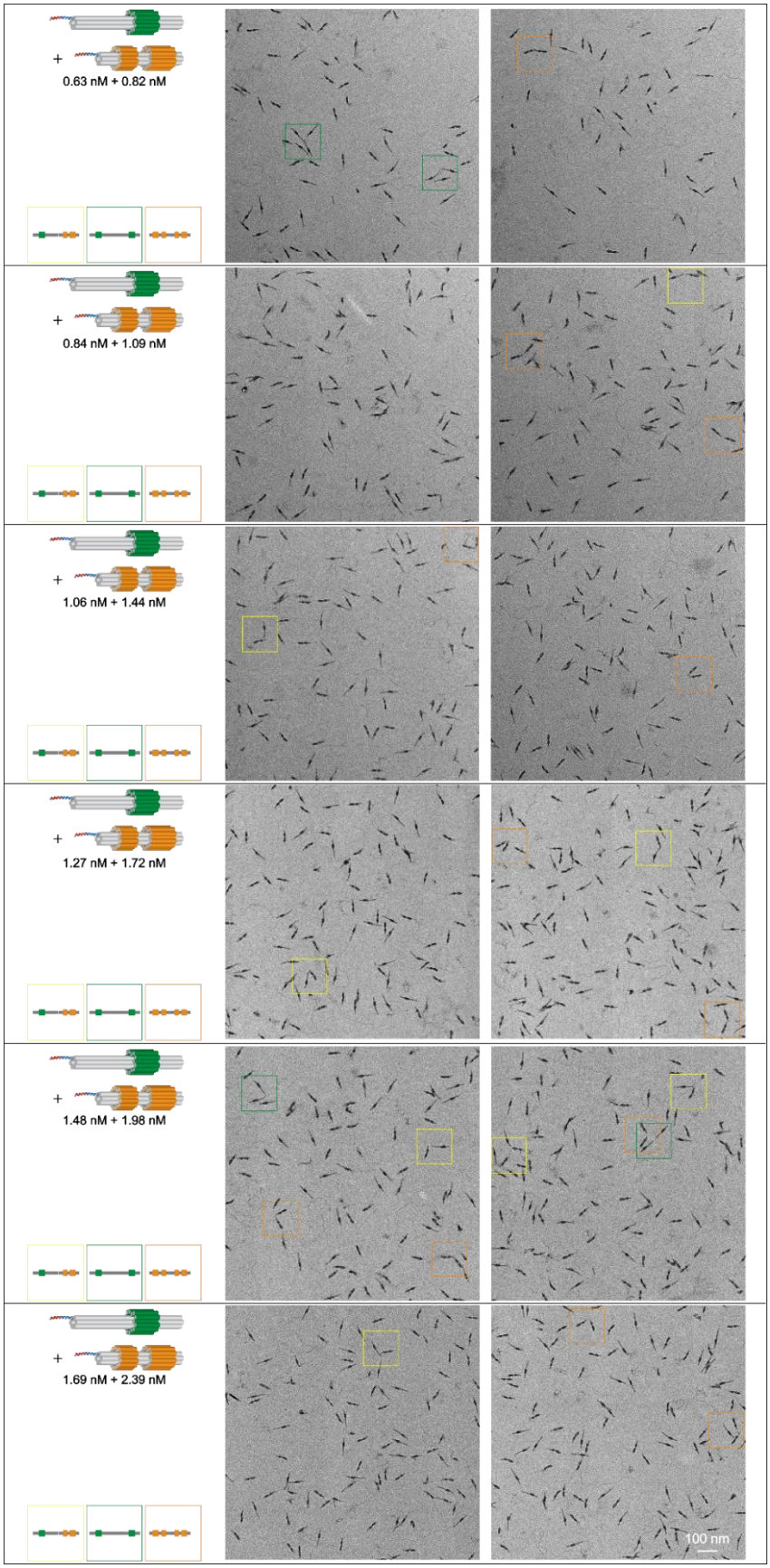

Figure S12-2 Representative TEM images of mixture of A_1 and B_1 at different initial concentrations.

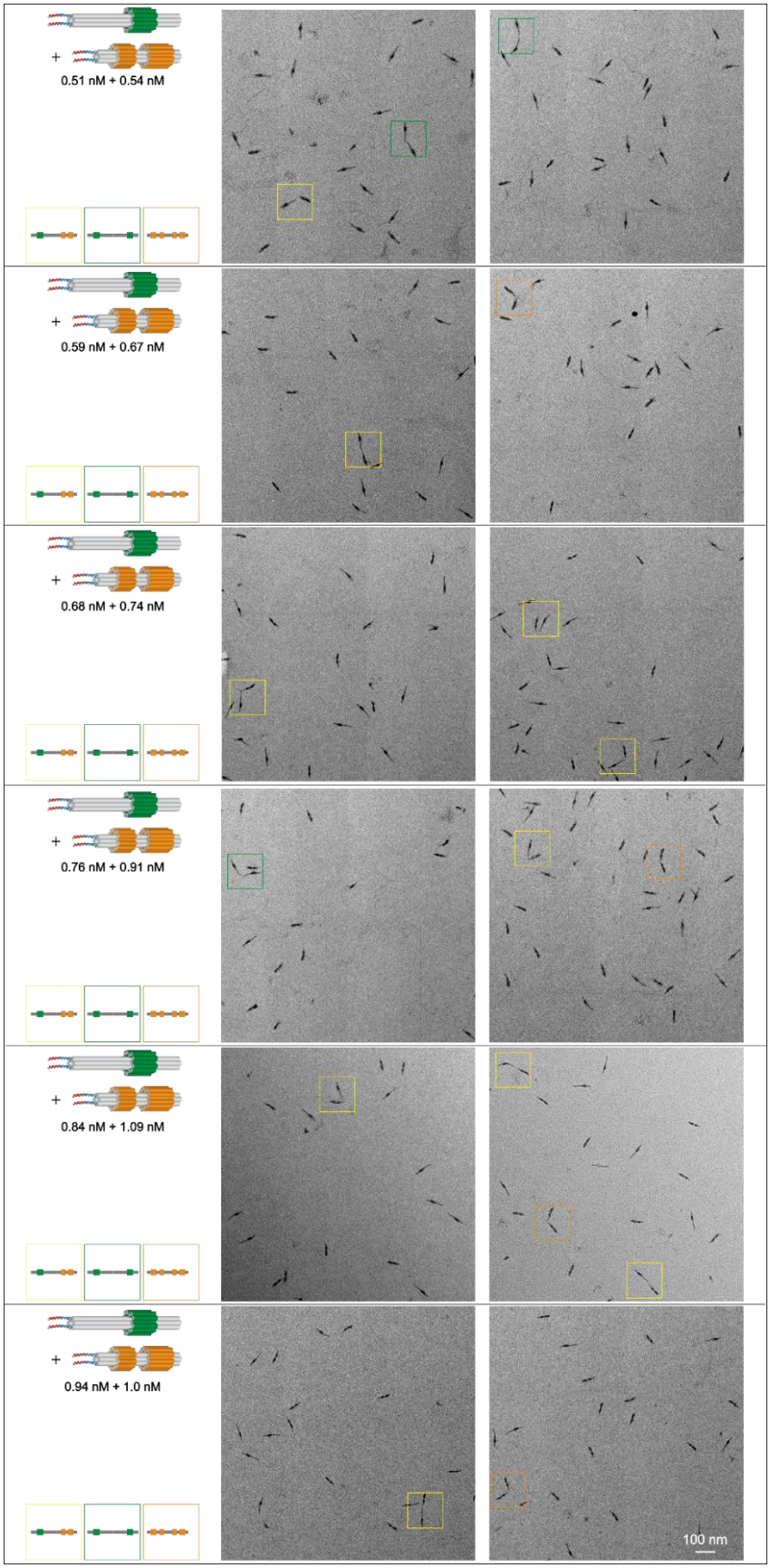

Figure S12-3 Representative TEM images of mixture of A_2 and B_2 at different initial concentrations.

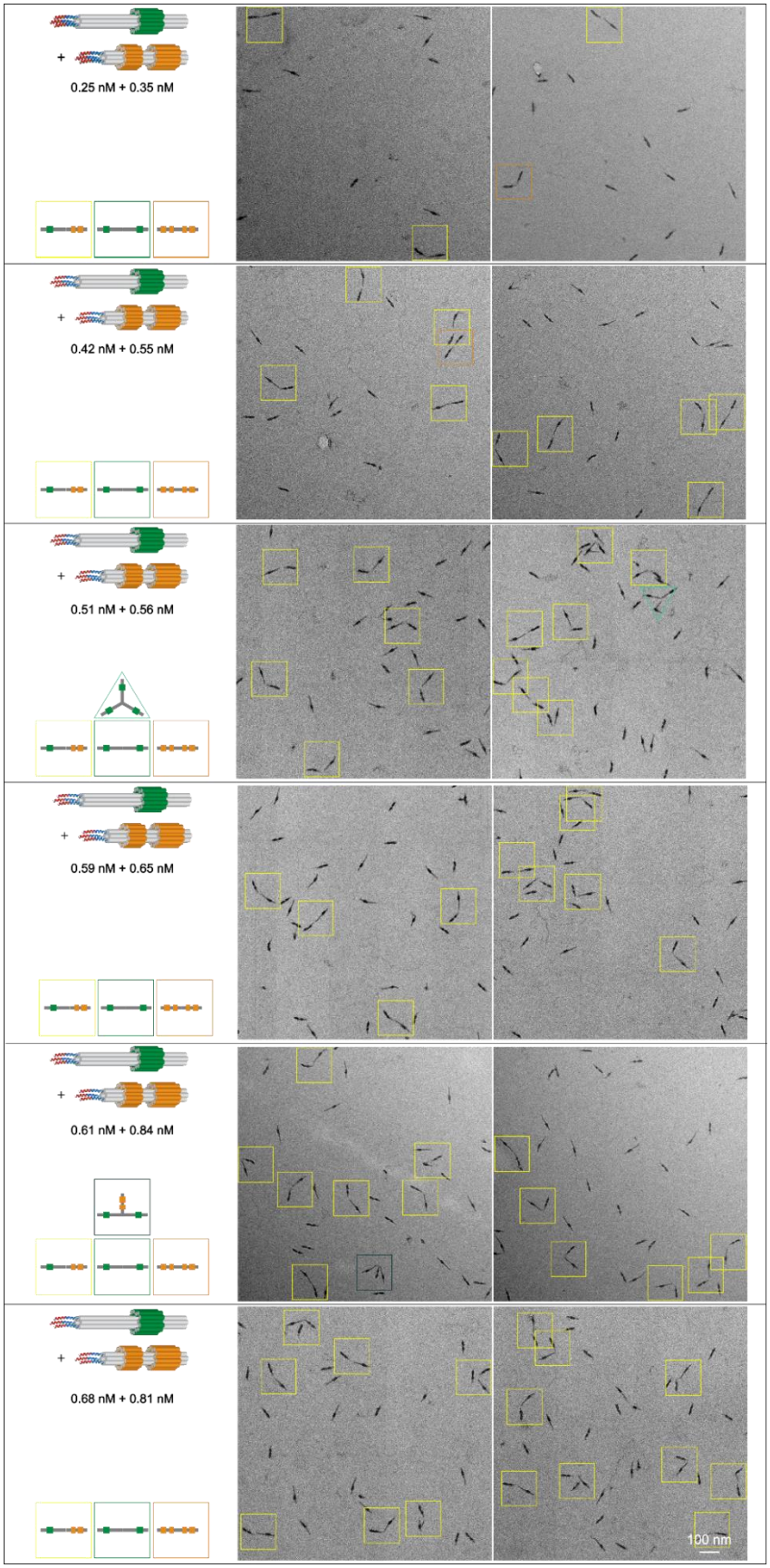

Figure S12-4 Representative TEM images of mixture of A_3 and B_3 at different initial concentrations.

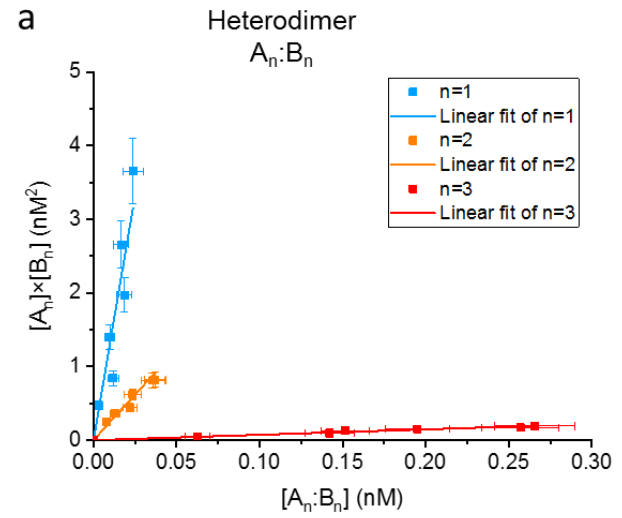

Fitting results:

n	Intercept Value	Intercept SE	Slope Value	Slope SE
1	0	0	132.9	17.3
2	0	0	24.8	2.5
3	0	0	0.74	0.05

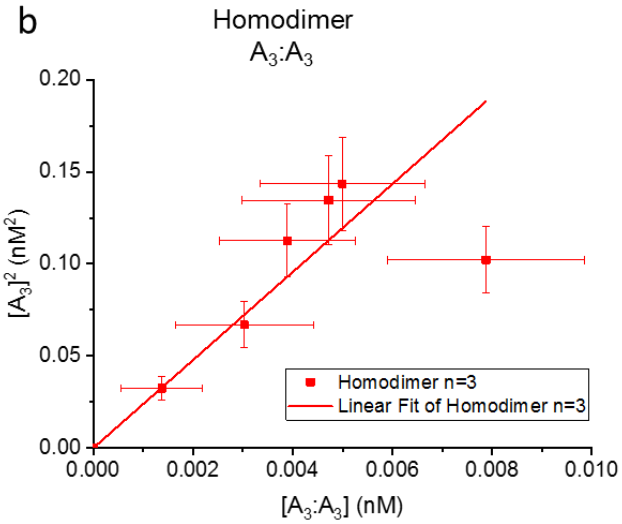

Fitting results:

n	Intercept Value	Intercept SE	Slope Value	Slope SE
3	0	0	23.9	4.1

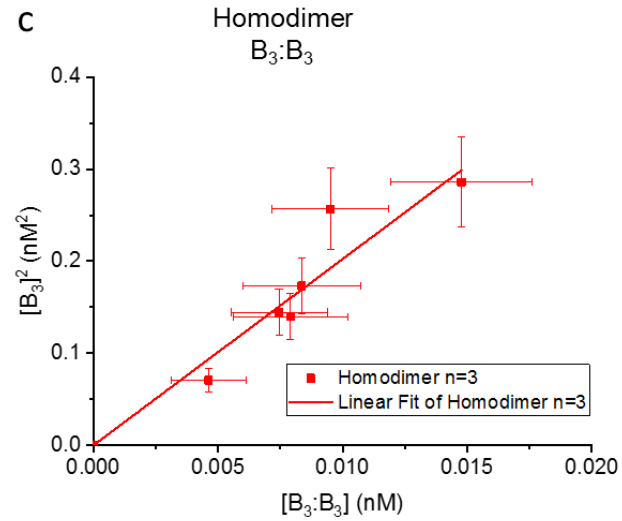

Fitting results:

n	Intercept Value	Intercept SE	Slope Value	Slope SE
3	0	0	20.2	2.6

Figure S13 Determination of K_ds by analysis of concentrations inferred from TEM images. (**a**) heterodimer A_n:B_n (n=1, 2, and 3) (as Figure 3e), (**b**) homodimer A_3:A_3, and (**c**) homodimer B_3:B_3. Left: Data and fits. Right: Fitting results.

Supporting Tables

Table S1 Sequences of designed heterodimeric coiled coils. Peptides were acetylated at the *N*-terminus and amidated at the *C*-terminus. Tryptophan or tyrosine chromophores were incorporated at 'f' positions to allow determination of peptide concentration. (Z=azidonorleucine)

Name	Sequence
	gabcdef gabcdef gabcdef gabcdef gabcdef gabcdef gabcdef gabcdef
CC-Di-EN4	Ac-G EIAALEQ EIAALEQ KNAALKW KIAALKQ G-NH_2
CC-Di-KN4	Ac-G KIAALKQ KIAALKY ENAALEQ EIAALEQ G-NH_2
CC-Di-EN3.5	Ac-G LEQ EIAALEQ KNAALKW KIAALKQ G-NH_2
CC-Di-KN3.5	Ac-G LKQ KIAALKY ENAALEQ EIAALEQ G-NH_2
CC-Di-EN3	Ac-G EIAALEQ KNAALKW KIAALKQ G-NH_2
CC-Di-KN3	Ac-G KIAALKY ENAALEQ EIAALEQ G-NH_2
CC-Di-EK	Ac-G EIAALEQ ENAALEQ KIAALKW KNAALKQ G-NH_2
CC-Di-KE	Ac-G KIAALKQ KNAALKY EIAALEQ ENAALEQ G-NH_2
CC-Di-EK-Z	Ac-G EIAALEQ ENAALEQ KIAALKW KNAALKQ GZ-NH_2
Z-CC-Di-KE	Ac-ZG KIAALKQ KNAALKY EIAALEQ ENAALEQ G-NH_2
CC-Di-EK-C | CC-Di-KE-C	Ac-G EIAALEQ ENAALEQ KIAALKW KNAALKQ GC-NH_2 | Ac-G KIAALKQ KNAALKY EIAALEQ ENAALEQ GC-NH_2
CC-Di-EK-C | C-CC-Di-KE	Ac-G EIAALEQ ENAALEQ KIAALKW KNAALKQ GC-NH_2 | Ac-CGG KIAALKQ KNAALKY EIAALEQ ENAALEQ G-NH_2

Table S2 Midpoints of thermal unfolding transitions for additional peptides in this study. Midpoints of thermal unfolding transitions were determined from the maxima of first order derivatives of the thermal profiles recorded at 222 nm by CD spectroscopy. Experimental conditions and unfolding data are in Figure S2.

Peptide(s)	T_M (±1 °C)
CC-Di-EN3:KN3	19
CC-Di-EN3.5:KN3.5	45
CC-Di-EN4	42
CC-Di-KN4	29
CC-Di-EN4:KN4	70
CC-Di-EK-C | CC-Di-KE-C	>95
CC-Di-EK-C | C-CC-Di-KE	67

Table S3. Peptide oligomeric states as determination by AUC. Calculated partial specific volumes (vbar) and molecular weights vs. AUC-determined molecular weights and consequent deduced oligomeric states for peptides in this study and for which the data are shown in Figure S3.

*Sample prepared with 10 fold excess of tris(2-carboxylethyl)phosphine hydrochloride (TCEP) reducing agent.
**Sample prepared with 5-fold excess of TCEP relative to total peptide concentration.
†N.B. *N*-terminally labelled C-CC-Di-EK exists as a dimer in solution even under reducing conditions.

	Peptide(s)	vbar (ccm/g)	Average MW_{calc} (Da)	MW_{AUC} (Da)	Oligomeric State	99% Confidence Limits (Da)	λ (nm)
a	CC-Di-EN3	0.76475	2493	2369	0.95 x monomer	2348–2390	280
b	CC-Di-EN3.5	0.76078	2863	2982	1.04 x monomer	2963–3001	280
c	CC-Di-EN4	0.76046	3248	6079	1.87 x monomer	6047–6110	280
d	CC-Di-EN3:KN3	0.75537	4965	3657	0.74 x dimer	3638–3676	280
e	CC-Di-EN3.5:KN3.5	0.75632	5704	5433	0.95 x dimer	5397–5442	280
f	CC-Di-EN4:KN4	0.75977	6474	6552	1.01 x dimer	6484–6621	280
g	CC-Di-EK	0.74973	3249	3274	1.00 x monomer	3258–3291	280
h	CC-Di-KE	0.74827	3226	3096	0.96 x monomer	3080–3114	235
i	CC-Di-EK:KE	0.74900	6474	6171	0.95 x dimer	6137–6205	280
j	*C-CC-Di-EK	0.74407	3409	6683	1.96 x monomer†	6636–6731	280
k	CC-Di-EK-C*	0.74591	3352	3474	1.04 x monomer	6636–6731	280
l	*C-CC-Di-KE	0.76264	3386	3126	0.92 x monomer	3107–3145	235
m	CC-Di-KE-C*	0.74447	3329	3062	0.92 x monomer	3043–3080	235
n	CC-Di-EK-C:KE-C reduced**	0.74519	6681	6166	0.92 x dimer	6144–6187	280
o	CC-Di-EK-C | CC-Di-KE-C	0.74519	6679	6695	1.00 x obligate dimer	6669–6722	280
p	CC-Di-EK-C | C-CC-Di-KE	0.74427	6736	17,610	2.6 x obligate dimer	17,549–17,679	280

Table S4-1 Equilibrium concentrations of different assemblies in mixtures of origamis A_0 and B_0. Each experiment corresponds to a mixture prepared with different initial concentrations (Conc(0)) of origamis A_0 and B_0. After equilibration, numbers of each assembly/complex (N) in TEM images were counted and corresponding equilibrium concentrations were calculated. The numbers of "dimers" observed are consistent with a random distribution of origami nanostructures in each micrograph with a minimum detectable separation between the ends of adjacent origamis of 8 nm: pairs of origamis with a closer separation are "false positives", counted as dimers but not linked by peptide-peptide interactions. Equilibrium concentrations shown here were calculated *without* deduction of this false positive background.

Experiment 1	A_0	B_0	A_0B_0	A_0A_0	B_0B_0	Sum	$N_{total}(A_0)$	$N_{total}(B_0)$
N	1089	1192	2	2	3		1095	1200
Ratio to $N_{total}(A_0)$	99.5%		0.2%	0.4%		100%		
Ratio to $N_{total}(B_0)$		99.3%	0.2%		0.5%	100%		
Conc(0)/nM	0.68	0.74						
Conc(etot)/nM	0.6721	0.7356	0.0012	0.0012	0.0019			

Experiment 2	A_0	B_0	A_0B_0	A_0A_0	B_0B_0	Sum	$N_{total}(A_0)$	$N_{total}(B_0)$
N	1178	1276	4	5	3		1192	1286
Ratio to $N_{total}(A_0)$	98.8%		0.3%	0.8%		100%		
Ratio to $N_{total}(B_0)$		99.2%	0.3%		0.5%	100%		
Conc(0)/nM	0.84	0.91						
Conc(etot)/nM	0.8348	0.9042	0.0028	0.0035	0.0021			

Experiment 3	A_0	B_0	A_0B_0	A_0A_0	B_0B_0	Sum	$N_{total}(A_0)$	$N_{total}(B_0)$
N	1302	1329	6	7	6		1322	1347
Ratio to $N_{total}(A_0)$	98.5%		0.5%	1.1%		100%		
Ratio to $N_{total}(B_0)$		98.7%	0.4%		0.9%	100%		
Conc(0)/nM	1.27	1.29						
Conc(etot)/nM	1.2479	1.2738	0.0058	0.0067	0.0058			

Experiment 4	A_0	B_0	A_0B_0	A_0A_0	B_0B_0	Sum	$N_{total}(A_0)$	$N_{total}(B_0)$
N	1910	2116	5	7	8		1929	2137
Ratio to $N_{total}(A_0)$	99.0%		0.3%	0.7%		100%		
Ratio to $N_{total}(B_0)$		99.0%	0.2%		0.7%	100%		
Conc(0)/nM	1.35	1.50						
Conc(etot)/nM	1.3382	1.4825	0.0035	0.0049	0.0056			

Experiment 5	A_0	B_0	A_0B_0	A_0A_0	B_0B_0	Sum	$N_{total}(A_0)$	$N_{total}(B_0)$
N	1259	1428	6	4	6		1273	1446
Ratio to $N_{total}(A_0)$	98.9%		0.5%	0.6%		100%		
Ratio to $N_{total}(B_0)$		98.8%	0.4%		0.8%	100%		
Conc(0)/nM	1.44	1.63						
Conc(etot)/nM	1.4202	1.6108	0.0068	0.0045	0.0068			

Experiment 6	A_0	B_0	A_0B_0	A_0A_0	B_0B_0	Sum	$N_{total}(A_0)$	$N_{total}(B_0)$
N	1671	1712	7	6	7		1690	1733
Ratio to $N_{total}(A_0)$	98.9%		0.4%	0.7%		100%		
Ratio to $N_{total}(B_0)$		98.8%	0.4%		0.8%	100%		
Conc(0)/nM	1.57	1.61						
Conc(etot)/nM	1.5535	1.5916	0.0065	0.0056	0.0065			

Table S4-2 Equilibrium concentrations of different assemblies in mixtures of origamis A_1 and B_1. Each experiment corresponds to a mixture prepared with different initial concentrations (Conc(0)) of origamis A_1 and B_1. After equilibration, numbers of each assembly/complex (N) in TEM images were counted and corresponding equilibrium concentrations were calculated before (Conc(etot)) and after (Conc(e)) correction for a background corresponding to random coincidences (N_{FP}).

Experiment 1	A_1	B_1	A_1B_1	A_1A_1	B_1B_1	$(B_1)_3$	Sum	$N_{total}(A_1)$	$N_{total}(B_1)$	n_m
N	1003	1239	8	9	30	6		1029	1325	21
Ratio to $N_{total}(A_1)$	97.50%		0.80%	1.70%			100%			
Ratio to $N_{total}(B_1)$		93.50%	0.60%		4.50%	1.40%	100%			
Conc(0)/nM	0.63	0.82								
Conc(etot)/nM	0.6175	0.7628	0.0049	0.0055	0.0185					
N_{FP}			2.90	1.17	1.79					
Conc(e)/nM	0.6175	0.7628	0.0031	0.0048	0.0174					

Experiment 2	A_1	B_1	A_1B_1	A_1A_1	B_1B_1	$(B_1)_3$	Sum	$N_{total}(A_1)$	$N_{total}(B_1)$	n_m
N	1003	1268	19	8	23	2		1038	1339	14
Ratio to $N_{total}(A_1)$	96.60%		1.80%	1.50%			100%			
Ratio to $N_{total}(B_1)$		94.70%	1.40%		3.40%	0.40%	100%			
Conc(0)/nM	0.84	1.09								
Conc(etot)/nM	0.8162	1.0319	0.0155	0.0065	0.0187					
N_{FP}			4.45	1.76	2.81					
Conc(e)/nM	0.8162	1.0319	0.0118	0.0051	0.0164					

Experiment 3	A_1	B_1	A_1B_1	A_1A_1	B_1B_1	$(B_1)_3$	$(B_1)_4$	$A_1(B_1)_2$	Sum	$N_{total}(A_1)$	$N_{total}(B_1)$	n_m
N	1026	1355	15	5	22	4	2	1		1052	1436	13
Ratio to $N_{total}(A_1)$	97.50%		1.40%	1.00%				0.10%	100%			
Ratio to $N_{total}(B_1)$		94.40%	1.00%		3.10%	0.80%	0.60%	0.10%	100%			
Conc(0)/nM	1.06	1.44										
Conc(etot)/nM	1.0298	1.36	0.0151	0.005	0.0221							
N_{FP}			5.24	1.98	3.46							
Conc(e)/nM	1.0298	1.3600	0.0098	0.0030	0.0186							

Experiment 4	A_1	B_1	A_1B_1	A_1A_1	B_1B_1	$(B_1)_3$	$(B_1)_4$	Sum	$N_{total}(A_1)$	$N_{total}(B_1)$	n_m
N	1182	1557	24	9	36	2	1		1224	1663	15
Ratio to $N_{total}(A_1)$	96.60%		2.00%	1.50%				100%			
Ratio to $N_{total}(B_1)$		93.60%	1.40%		4.30%	0.40%	0.20%	100%			
Conc(0)/nM	1.27	1.72									
Conc(etot)/nM	1.2236	1.6118	0.0248	0.0093	0.0373						
N_{FP}			6.01	2.28	3.96						
Conc(e)/nM	1.2236	1.6118	0.0186	0.0070	0.0332						

Experiment 5	A_1	B_1	A_1B_1	A_1A_1	B_1B_1	$(B_1)_3$	$(A_1)_2B_1$	Sum	$N_{total}(A_1)$	$N_{total}(B_1)$	n_m
N	1103	1457	19	13	29	3	1		1150	1544	13
Ratio to $N_{total}(A_1)$	95.90%		1.70%	2.30%			0.20%	100%			
Ratio to $N_{total}(B_1)$		94.40%	1.20%		3.80%	0.60%	0.10%	100%			
Conc(0)/nM	1.48	1.98									
Conc(etot)/nM	1.4178	1.8728	0.0244	0.0167	0.0373						
N_{FP}			6.06	2.29	4.00						
Conc(e)/nM	1.4178	1.8728	0.0166	0.0138	0.0321						

Experiment 6	A_1	B_1	A_1B_1	A_1A_1	B_1B_1	$(B_1)_3$	$(B_1)_4$	Sum	$N_{total}(A_1)$	$N_{total}(B_1)$	n_m
N	1028	1424	21	10	31	1	1		1069	1514	12
Ratio to $N_{total}(A_1)$	96.20%		2.00%	1.90%				100%			
Ratio to $N_{total}(B_1)$		94.10%	1.40%		4.10%	0.20%	0.30%	100%			
Conc(0)/nM	1.69	2.39									
Conc(etot)/nM	1.6246	2.2504	0.0332	0.0158	0.049						
N_{FP}			5.98	2.16	4.14						
Conc(e)/nM	1.6246	2.2504	0.0237	0.0124	0.0424						

Table S4-3 Equilibrium concentrations of different assemblies in mixtures of origamis A_2 and B_2. Each experiment corresponds to a mixture prepared with different initial concentrations (Conc(0)) of origamis A_2 and B_2. After equilibration, numbers of each assembly/complex (N) in TEM images were counted and corresponding equilibrium concentrations were calculated before (Conc(etot)) and after (Conc(e)) correction for a background corresponding to random coincidences (N_{FP}).

Experiment 1	A_2	B_2	A_2B_2	A_2A_2	B_2B_2	$(A_2)_3$	$(A_2)_4$	Sum	$N_{total}(A_2)$	$N_{total}(B_2)$	n_m
N	948	1006	16	8	12	1	1		987	1046	45
Ratio to $N_{total}(A_2)$	96.00%		1.60%	1.60%		0.30%	0.40%	100%			
Ratio to $N_{total}(B_2)$		96.20%	1.50%		2.30%			100%			
Conc(0)/nM	0.51	0.54									
Conc(etot)/nM	0.4868	0.5166	0.0082	0.0041	0.0062						
N_{FP}			1.04	0.49	0.55						
Conc(e)/nM	0.4868	0.5166	0.0077	0.0039	0.0059						

Experiment 2	A_2	B_2	A_2B_2	A_2A_2	B_2B_2	$(A_2)_3$	$(A_2)_6$	Sum	$N_{total}(A_2)$	$N_{total}(B_2)$	n_m
N	833	951	20	5	11	1	1		872	993	50
Ratio to $N_{total}(A_2)$	95.50%		2.30%	1.10%		0.30%	0.70%	100%			
Ratio to $N_{total}(B_2)$		95.80%	2.00%		2.20%			100%			
Conc(0)/nM	0.59	0.67									
Conc(etot)/nM	0.5648	0.6449	0.0136	0.0034	0.0075						
N_{FP}			0.78	0.34	0.44						
Conc(e)/nM	0.5648	0.6449	0.0130	0.0032	0.0072						

Experiment 3	A_2	B_2	A_2B_2	A_2A_2	B_2B_2	$(A_2)_8$	$A_2(B_2)_3$	$A_2(B_2)_4$	Sum	$N_{total}(A_2)$	$N_{total}(B_2)$	n_m
N	902	983	32	5	11	1	1	2		955	1048	40
Ratio to $N_{total}(A_2)$	94.50%		3.40%	1.00%		0.80%	0.10%	0.20%	100%			
Ratio to $N_{total}(B_2)$		93.80%	3.10%		2.10%	0.10%	0.30%	0.80%	100.10%			
Conc(0)/nM	0.68	0.74										
Conc(etot)/nM	0.6383	0.6956	0.0226	0.0035	0.0078							
N_{FP}			1.09	0.50	0.59							
Conc(e)/nM	0.6383	0.6956	0.0219	0.0032	0.0074							

Experiment 4	A_2	B_2	A_2B_2	A_2A_2	B_2B_2	$(B_2)_4$	$A_2(B_2)_2$	$(A_2)_2B_2$	Sum	$N_{total}(A_2)$	$N_{total}(B_2)$	n_m
N	802	959	27	7	10	1	2	1		847	1015	47
Ratio to $N_{total}(A_2)$	94.70%		3.20%	1.70%			0.20%	0.20%	100%			
Ratio to $N_{total}(B_2)$		94.50%	2.70%		2.00%	0.40%	0.40%	0.10%	100%			
Conc(0)/nM	0.76	0.91										
Conc(etot)/nM	0.7198	0.8608	0.0242	0.0063	0.009							
N_{FP}			0.80	0.34	0.48							
Conc(e)/nM	0.7198	0.8608	0.0235	0.0060	0.0085							

Experiment 5	A_2	B_2	A_2B_2	A_2A_2	B_2B_2	$(B_2)_3$	$(A_2)_3(B_2)_2$	Sum	$N_{total}(A_2)$	$N_{total}(B_2)$	n_m
N	655	843	30	3	8	1	2		697	896	50
Ratio to $N_{total}(A_2)$	94.00%		4.30%	0.90%			0.90%	100%			
Ratio to $N_{total}(B_2)$		94.10%	3.30%		1.80%	0.30%	0.40%	100%			
Conc(0)/nM	0.84	1.09									
Conc(etot)/nM	0.7938	1.0216	0.0364	0.0036	0.0097						
N_{FP}			0.54	0.21	0.35						
Conc(e)/nM	0.7938	1.0216	0.0357	0.0034	0.0093						

Experiment 6	A_2	B_2	A_2B_2	A_2A_2	B_2B_2	$(A_2)_3$	$(B_2)_3$	$(A_2)_3B$	Sum	$N_{total}(A_2)$	$N_{total}(B_2)$	n_m
N	968	1036	42	10	11	3	1	1		1042	1104	47
Ratio to $N_{total}(A_2)$	92.90%		4.00%	1.90%		0.90%		0.30%	100%			
Ratio to $N_{total}(B_2)$		93.80%	3.80%		2.00%		0.30%	0.10%	100%			
Conc(0)/nM	0.94	1										
Conc(etot)/nM	0.875	0.9364	0.038	0.009	0.0099							
N_{FP}			1.05	0.49	0.56							
Conc(e)/nM	0.8750	0.9364	0.0370	0.0086	0.0094							

Table S4-4 Equilibrium concentrations of different assemblies in mixtures of origamis A_3 and B_3. Each experiment corresponds to a mixture prepared with different initial concentrations (Conc(0)) of origamis A_3 and B_3. After equilibration, numbers of each assembly/complex (N) in TEM images were counted and corresponding equilibrium concentrations were calculated before (Conc(etot)) and after (Conc(e)) correction for a background corresponding to random coincidences (N_{FP}).

Experiment 1	A_3	B_3	A_3B_3	A_3A_3	B_3B_3	$(A_3)_3$	$(A_3)_5$	$(B_3)_3$	$(B_3)_4$	$(A_3)_2B_3$	$A_3(B_3)_2$	Sum	$N_{total}(A_3)$	$N_{total}(B_3)$	n_m
N	382	564	133	3	10	2	1	1	2	2	2		538	734	43
Ratio to $N_{total}(A_3)$	71.00%		24.70%	1.10%		1.10%	0.90%			0.70%	0.40%	100%			
Ratio to $N_{total}(B_3)$		76.80%	18.10%		2.70%			0.40%	1.10%	0.30%	0.50%	100%			
Conc(0)/nM	0.25	0.35													
Conc(etot)/nM	0.1799	0.2657	0.0626	0.0014	0.0047										
N_{FP}			0.25	0.08	0.18										
Conc(e)/nM	0.1799	0.2657	0.0625	0.0014	0.0046										

Experiment 2	A_3	B_3	A_3B_3	A_3A_3	B_3B_3	$(A_3)_3$	$(A_3)_5$	$(B_3)_3$	$(A_3)_2B_3$	$A_3(B_3)_2$	$(A_3)_2(B_3)_2$	Sum	$N_{total}(A_3)$	$N_{total}(B_3)$	n_m
N	418	604	230	5	13	1	2	3	2	4	2		683	883	39
Ratio to $N_{total}(A_3)$	61.20%		33.70%	1.50%		0.40%	1.50%		0.60%	0.60%	0.60%	100%			
Ratio to $N_{total}(B_3)$		68.40%	26.00%		2.90%			1.00%	0.20%	0.90%	0.50%	100%			
Conc(0)/nM	0.42	0.55													
Conc(etot)/nM	0.2585	0.3735	0.1422	0.0031	0.008										
N_{FP}			0.32	0.11	0.23										
Conc(e)/nM	0.2585	0.3735	0.1420	0.0030	0.0079										

Experiment 3	A_3	B_3	A_3B_3	A_3A_3	B_3B_3	$(A_3)_3$	$(A_3)_6$	$(B_3)_3$	$(B_3)_{10}$	$A_3(B_3)_2$	$(A_3)_2B_3$	Sum	$N_{total}(A_3)$	$N_{total}(B_3)$	n_m
N	742	841	336	9	17	2	2	3	1	5	1		1121	1241	34
Ratio to $N_{total}(A_3)$	66.20%		30.00%	1.60%		0.50%	1.10%			0.40%	0.20%	100%			
Ratio to $N_{total}(B_3)$		67.80%	27.10%		2.70%			0.70%	0.80%	0.80%	0.10%	100%			
Conc(0)/nM	0.51	0.56													
Conc(etot)/nM	0.3355	0.3802	0.1519	0.0041	0.0077										
N_{FP}			0.90	0.40	0.51										
Conc(e)/nM	0.3355	0.3802	0.1515	0.0039	0.0075										

Experiment 4	A_3	B_3	A_3B_3	A_3A_3	B_3B_3	$(A_3)_3$	$(A_3)_5$	$(A_3)_7$	$(B_3)_3$	$(B_3)_4$	$A_3(B_3)_2$	$A_3(B_3)_3$	$(A_3)_2B_3$	Sum	$N_{total}(A_3)$	$N_{total}(B_3)$	n_m
N	597	677	318	8	14	1	1	1	1	1	7	1	4		962	1051	27
Ratio to $N_{total}(A_3)$	62.10%		33.10%	1.70%		0.30%	0.50%	0.70%			0.70%	0.10%	0.80%	100%			
Ratio to $N_{total}(B_3)$		64.40%	30.30%		2.70%				0.30%	0.40%	1.30%	0.30%	0.40%	100%			
Conc(0)/nM	0.59	0.65															
Conc(etot)/nM	0.3669	0.4161	0.1955	0.0049	0.0086												
N_{FP}			0.73	0.32	0.42												
Conc(e)/nM	0.3669	0.4161	0.1950	0.0047	0.0083												

Experiment 5	A_3	B_3	A_3B_3	A_3A_3	B_3B_3	$(A_3)_3$	$(A_3)_6$	B3	$(B_3)_4$	$A_3(B_3)_2$	$(A_3)_2B_3$	Sum	$N_{total}(A_3)$	$N_{total}(B_3)$	n_m
N	719	1203	579	18	34	1	1	6	3	5	10		1368	1900	45
Ratio to $N_{total}(A_3)$	52.60%		42.30%	2.60%		0.20%	0.40%			0.40%	1.50%	100%			
Ratio to $N_{total}(B_3)$		63.30%	30.50%		3.60%			0.90%	0.60%	0.50%	0.50%	100%			
Conc(0)/nM	0.61	0.84													
Conc(etot)/nM	0.3197	0.5348	0.2574	0.008	0.0151										
N_{FP}			0.94	0.28	0.79										
Conc(e)/nM	0.3197	0.5348	0.2570	0.0079	0.0148										

Experiment 6	A_3	B_3	A_3B_3	A_3A_3	B_3B_3	$(A_3)_3$	$(A_3)_6$	$(A_3)_7$	$(B_3)_3$	$A_3(B_3)_2$	$A_3(B_3)_3$	$(A_3)_2B_3$	$(A_3)_3B_3$	Sum	$N_{total}(A_3)$	$N_{total}(B_3)$	n_m
N	729	975	512	10	19	1	1	1	3	8	2	5	1		1300	1562	33
Ratio to $N_{total}(A_3)$	56.10%		39.40%	1.50%		0.20%	0.50%	0.50%		0.60%	0.20%	0.80%	0.20%	100%			
Ratio to $N_{total}(B_3)$		62.40%	32.80%		2.40%				0.60%	1.00%	0.40%	0.30%	0.10%	100%			
Conc(0)/nM	0.68	0.81															
Conc(etot)/nM	0.3789	0.5068	0.2661	0.0052	0.0099												
N_{FP}			1.06	0.39	0.71												
Conc(e)/nM	0.3789	0.5068	0.2656	0.0050	0.0095												

Table S5 Data and corresponding uncertainties used for linear fits to determine K_ds. Quantities ($[A_n:B_n]$, $[A_n]\times[B_n]$, $[A_n:A_n]$, $[A_n]^2$, $[B_n:B_n]$, and $[B_n]^2$, valences n=1, 2 and 3) were calculated from data in Table S4. Uncertainties (Err) were calculated as discussed in Supporting Discussions.

n=1	$[A_1:B_1]$	Err $[A_1:B_1]$	$[A_1]\times[B_1]$	Err $[A_1]\times[B_1]$	$[A_1:A_1]$	Err $[A_1:A_1]$	$[A_1]^2$	Err $[A_1]^2$	$[B_1:B_1]$	Err $[B_1:B_1]$	$[B_1]^2$	Err $[B_1]^2$
Experiment 1	0.0031	0.0013	0.4711	0.0569	0.0048	0.0018	0.3813	0.0656	0.0174	0.0035	0.5819	0.0988
Experiment 2	0.0118	0.0032	0.8422	0.1017	0.0051	0.0020	0.6662	0.1146	0.0164	0.0039	1.0648	0.1806
Experiment 3	0.0098	0.0030	1.4005	0.1687	0.0030	0.0016	1.0604	0.1821	0.0186	0.0045	1.8496	0.3125
Experiment 4	0.0186	0.0045	1.9721	0.2357	0.0070	0.0027	1.4971	0.2549	0.0332	0.0064	2.5978	0.4360
Experiment 5	0.0166	0.0046	2.6553	0.3186	0.0138	0.0043	2.0102	0.3437	0.0321	0.0069	3.5076	0.5905
Experiment 6	0.0237	0.0062	3.6561	0.4399	0.0124	0.0044	2.6393	0.4533	0.0424	0.0088	5.0644	0.8536

n=2	$[A_2:B_2]$	Err $[A_2:B_2]$	$[A_2]\times[B_2]$	Err $[A_2]\times[B_2]$	$[A_2:A_2]$	Err $[A_2:A_2]$	$[A_2]^2$	Err $[A_2]^2$	$[B_2:B_2]$	Err $[B_2:B_2]$	$[B_2]^2$	Err $[B_2]^2$
Experiment 1	0.0077	0.0021	0.2515	0.0306	0.0039	0.0014	0.2370	0.0409	0.0059	0.0018	0.2669	0.0459
Experiment 2	0.0130	0.0031	0.3642	0.0447	0.0032	0.0015	0.3190	0.0556	0.0072	0.0023	0.4158	0.0718
Experiment 3	0.0219	0.0043	0.4440	0.0542	0.0032	0.0015	0.4074	0.0706	0.0074	0.0024	0.4838	0.0833
Experiment 4	0.0235	0.0050	0.6196	0.0761	0.0060	0.0024	0.5182	0.0906	0.0085	0.0028	0.7409	0.1278
Experiment 5	0.0357	0.0072	0.8110	0.1010	0.0034	0.0020	0.6301	0.1122	0.0093	0.0034	1.0437	0.1818
Experiment 6	0.0370	0.0065	0.8193	0.0997	0.0086	0.0029	0.7655	0.1320	0.0094	0.0030	0.8769	0.1505

n=3	$[A_3:B_3]$	Err $[A_3:B_3]$	$[A_3]\times[B_3]$	Err $[A_3]\times[B_3]$	$[A_3:A_3]$	Err $[A_3:A_3]$	$[A_3]^2$	Err $[A_3]^2$	$[B_3:B_3]$	Err $[B_3:B_3]$	$[B_3]^2$	Err $[B_3]^2$
Experiment 1	0.0625	0.0074	0.0478	0.0063	0.0014	0.0008	0.0324	0.0061	0.0046	0.0015	0.0706	0.0128
Experiment 2	0.1420	0.0147	0.0965	0.0125	0.0030	0.0014	0.0668	0.0125	0.0079	0.0023	0.1395	0.0250
Experiment 3	0.1515	0.0147	0.1276	0.0158	0.0039	0.0014	0.1125	0.0198	0.0075	0.0019	0.1446	0.0252
Experiment 4	0.1950	0.0191	0.1527	0.0193	0.0047	0.0017	0.1346	0.0242	0.0083	0.0024	0.1732	0.0307
Experiment 5	0.2570	0.0232	0.1710	0.0210	0.0079	0.0020	0.1022	0.0180	0.0148	0.0028	0.2860	0.0486
Experiment 6	0.2656	0.0243	0.1921	0.0237	0.0050	0.0017	0.1436	0.0253	0.0095	0.0023	0.2569	0.0443

Table S6-1 DNA staple sequences: origami A

Name	Sequence
A MID-1	AAAAGCGTTAACCTGAGCGGATACATATTACTTTCTCATCAT
A MID-2	CCAACGAGGTGAAATTTTCAATATTATTAAATGCCTACGGGA
A MID-3	ACGCGCTTGTCAGCAGATATACGAGTTATCCGCTCACAAGCGTAATGTC
A MID-4	TAATTGTGTGGCCTCAGTTACCTTCGGAGATTATCCTTGGTC
A MID-5	AGATGCTAAAGTGCACCAGCGTTTCTGGGTCTCATATAAAAA
A MID-6	TGAGAATGCGTCAAGCAAAAAAGGGAATTCTTCCTACCTCTG
A MID-7	TACGGGATTGGTATGGCTTCACAGCTCCTTGAATA
A MID-8	ATACCTATTTCTACGGGGCAGAATCGGCGAGCGGTATCAGCTCGGTTGC
A MID-9	AGATTGTTGCGTTCGGTACGAACCCCCCGTT
A MID-10	CGGGCACCTAGAACGAAAACTCACTCCGGCAAGGTATG
A MID-11	AGGGCCGGAGTAAAAAAAAGGATCTTCACTGAAGCAACTACG
A MID-12	TGGAAAATCATGCCCCTTCGGTCCTCCGGAAACCATATTTAG
A MID-13	TAATACCCAACCAAGAGTTACATGATCCATCACGATTATCAG
A MID-14	TGACAGTACCAGCCAAGCTAGAGTAAGTTGCTACATTGGTAG
A MID-15	CATCTTTTTGAATGTTATTATCATGACAGTTAGCTATCCGTA
A MID-16	GAAGGCAGAAGCATGGCCCTTTCGTCACTCAAGGCGTCATTC
A MID-17	TTCGTTCATCGCGTTGCCTCAAGTCATCTTCGCTATTAGCGATTA
A MID-18	ACGGGTAGCGGGTAACACTTATCGCTTATCCGGTAACTTGTGTGCGTAG
A MID-19	GTCATGAAAAAGAGGAGTTCTTGAAGTGTGCCGGGAGCCGGA
A MID-20	AAAAATACAACTGACGGGGCGAAAACTCCACTGCATCAGAAG
A MID-21	GGTTATTGTGAGCAATAGCAGAACTTTATTTCTGTTGTGCAA
A MID-22	CTCATACAAGGGCGGTTGCTCTTGCCCGAGTGTATCCGGTTC
A MID-23	CTCTTGAGTTAAGGGCTTAATCAGTGAGCTCCAGACAGTTAA
A MID-24	CGTCTAAATCGTTGTAATTCTCTTACTGCGTTCTTTCTTCAG
A MID-25	TAGGCGTCCCATGTGACTGGTGAGTACTGCGCCACAAAACAG
A MID-26	ACACATGTTCAGCTGCGGCGACCTACGA
A MID-27	GGATGGCACAGGCATGCTGCATCCTGTTGGTGGCGAAACCCGATCGACGTGGC
A MID-28	ACTGTGGTTTGGCGGTTCGTTCGGCTTGTGT
A MID-29	TAGGCGGAGTTCGCTTTATCAGCAATAATACCAATGATTTTG
A MID-30	CCGCACATTAGGGGTGCCTAATGAACACAACTACGCGCAGAAATGCGGAGAC
A MID-31	CGAGGATTAGCGCAACGCCCACGCTGGAAGCTATAAAGATACCAGGC
A MID-32	CCAACCCGGTAAAAACCTGTCGTG
A MID-33	GTCAGCGGGCGGCATCAGAGC
A MID-34	GGCGACCGCTGCGCCCACTGGACTGCCCGCGCGGGGAAGTGT
A MID-35	CAGCCGGCGGTAGGTATCTCACATTGCTAGCC
A MID-36	AAGCTGGGCATCGTCTTGAGT
A MID-37*	**AGATTGTACTGAAGATGCGTAAGG**
A MID-38	GTCCGTGGCGTGTCCGCCTTTCTCTTCCCCCTCAC
A MID-39	ACGCTGTCCCTGCCGCTTACCTGCGCTCATG
A MID-40	TTCGGGAAGGTTCGCTTAGTTTGCAGAGCGAACAAACTCTTCCGCTTCC
A MID-41	AGAAAATACCGCATCAGGCGCCATGAGTGAAATACCGCACGAGTGCAGTC
A MID-42	ATTCAGGCCATCTGGCCTGACAGAAGATCTCTAGACATGGTCATAGCTG
A MID-43	CTCGGGATACCCTTTCTCATAGCTC
A MID-44	TGGGAAGGGCGATCGGTGCGGGCCGACCTCGCC
A MID-45	CCTGACGAGCATCACAAAAACAGGACTCC
A MID-46	AGTTGCCCATAGTTGCCCCAGTCGTGGTCCATATGCTGGCTTAACTATGTGTTGGCAAGC
A MID-47	GTTAGGAACCGATAACGCAGGAAATTATCCATCTG
A MID-48	AAAAGGCCAGCAAAAGGCCTTTCCATGATCTGTCGCG
A MID-49	TGCAGGCAAAAAAGGATCTCATCCCCGTCTGCAAGCGCCAGCTGGCGAAAG
A MID-50	GACCACGACGGGTTTTCCCAGTCACGGATGTGCGTGTAGATAACGAACACGGA
A MID-51	GCGGTAATACGGGAACATGTGAGC
A MID-52	TTTTTTGCAAGCTTG
A MID-53	TTTCCGCAGTACCCGGGGATCCCTTTGATGCAAGCTGTAAGC
A MID-54	GAAATTGCCGGAAGCATAAGATTTTGTTTCTT
A MID-55	TCGCTCACTGACTCGCTGCGCTCACTCAAAG
A MID-56	GTATGGCCAACGCTTTCCAGTCGGGGACA
A MID-57	AAAGCCTATTGCGTTGCGCTCCACCGGGAGCAGACGGGTGTC
A MID-58	CCAGCTGCATTAATGAATCTGGGCGCCACCGCTCTCAGTGTCTCAGCAGGCTCCGCCCC
A MID-59	GAGCTAACTTCAGGGCGGTCACATCGTCGTGGGCTTACTGCGCAACTGT
A LEFT-0 handle	TAAGTTGGCCGCAGTGTTAGAATCTGACGACCACCACTACTC
A LEFT-1	TTTTTCACTCATGGTTATGGCAG
A LEFT-2 handle	TCAAGGATCTTACCGCTGTTGAGGAATCTGACGACCACCACTACTC
A LEFT-3	TTTTATCCAGTTCGATGTAACCCACTC
A LEFT-4 handle	GTGCACCAACAAATAGGGGTTCCGCGCACAGAATCTGACGACCACCACTACTC
A LEFT-5	TTTTTTTCCCCGAAAAGTGCCACCTGA

A RIG-1	TTTTTTATCCGCCTAGAAGAACAGTTTTT
A RIG-2	TTTTTTTGAAGTTTT
A RIG-3	TTTTATTTGGTATCTGCGCTCTGCCTAGATTCTAAAGTATATATAGCGCAGAGTCTAT
A RIG-4	GCTACACTCCATCCAAGTGGTCCTGCAAAAATCAACCTTTTAAATTAAAAATTTT
A LEFT-0 ctrl	TAAGTTGGCCGCAGTGTTACGTTTTGACTACCTTCCTCCCCG
A LEFT-2 ctrl	TCAAGGATCTTACCGCTGTTGAGCGTTTTGACTACCTTCCTCCCCG
A LEFT-4 ctrl	GTGCACCAACAAATAGGGGTTCCGCGCACACGTTTTGACTACCTTCCTCCCCG
tag α ctrl	TTTTTTTTCGGGGAGGAAGGTAGTCAAAACG
tag α	TTTTTTTTGAGTAGTGGTGGTCGTCAGATTC

Note: * = 5’ end was modified with fluorophore Cy3. Handles and dummy control sequences are highlighted.

Table S6-2 DNA staple sequences: origami B

Name	Sequence
B MID-1	ACAGCCAGCCGATGCGTAACCCAACTGATCTTGAT
B MID-2	TTCTGGCAGCCTGACGTATAAAAATAACATGCAGCTCCCGGAG
B MID-3	ATTTATGAGTGACCCACGCTCACCTTACGCCCACCGCTGGAAGATGCTTTTCGGGCCTC
B MID-4	TCTAGTTACCAGTGCTGTCATGGTGGGGATCCTCTAGAAATT
B MID-5	ATTAAAAAGGTCAAGTCCAAAAGGCCCTCCGCCCCCCTGACGA
B MID-6	TCAGAGGCACGAGGGCTGCCTTATAGACACGACTTATC
B MID-7	TCCGTTAAAGTTTTAAGTCGTTTGGTATTTACTGTCATGCCA
B MID-8	GCAATACGGTAACATGTGAGCAAAAGGCCAGAGTCAAAGGCGGTAGATT
B MID-9	ACGTTGGTAGCTGCAAGGCGATACTGGCCCCAATGCTTAAAGTGTCACTGCCCGTGTCC
B MID-10	CAACAGTTACTTGAAGTGTATGTACTGGTAACAGGATTAG
B MID-11	CGACCGATTGGCCGATGATCCCCCATGTAGTAGTTTCCGCCT
B MID-12	TTCTGAGATGGTTACCAACGACGGGTGTGTATTTAGAAAAATAA
B MID-13	TCCGGCAGTTTGCAGATCCTTAACGCGCTGCCAGCTGCATTAAT
B MID-14	AAAAGAGCGCAGAAATCAAAATGCGTATTTCCAGTCGGGAAATTGCGCTAAAG
B MID-15	CAGAACTAACTTTACGCCAGTTAATAGTGAGTTACCAGTGTT
B MID-16	AGGGCGAAAACCAGGCATCGTCGGAAATTTATTGTCTGCAGATT
B MID-17	TTCGCTAGGCTCCACAATCTAAAGTATAAAAAATGGCGGTGG
B MID-18	GGCTGCGCAACTGTTCCCCACTCGTCCATTCA
B MID-19	CAGAGCGAGGGTGGCCGATACGGCTATCTCTCATAGCTCCCTTCGGGAAGCGT
B MID-20	CGCTGTTGAGATCCAGTTCCAGCATCTTTTA
B MID-21	GTAAGGGGCGAAAACTCTCATTGGACGAGCGCACGTTGTCTCTTCCTTTTT
B MID-22	TGTAAAACGACGGCCAGTGGTCGACCTGCAG
B MID-23	CGACGCCAGGGTTTTCCGAAAGGGACCGCGAAAACTTGCTAATGAGTGAG
B MID-24	TCAGGCGCCATTCGGCAGGAGAAGTGTGAATAAGGGCGAGAGTGCA
B MID-25	GCCACCCCACCCGACCGCTGCTACCATCAGAGTTCCTTCGGA
B MID-26	TGAGTCCAACCCGGTACCGGTAAGCTG
B MID-27	CTTTCACCAGCGTTTCTAGGAAGGGCAAACGTTCAAGTCA
B MID-28	GCATGCAAGCTTGAAATTGTTATC
B MID-29	CCATATGCGAATACCGCAGCAATTCGGTGCTGTGACT
B MID-30	TTCAGTAGCCGGAAGCTATCTCAGTTCGGCACGAACCCCCCG
B MID-31	TGTGTGTAGGTCGTTCGCGCTTTCAGCGATCCACGTTACTTTGAT
B MID-32	CCAAGCTGGCTATCGTTAACTACTAACTACCGCTCTG
B MID-33	AAGGCAAAATGCCGCAAAAACTCATATGCCATTCCGG
B MID-34	CGCTCACAATTCCACACAAGGGGTGCGTCTGACTCACCTAAGCA
B MID-35	AATAAGGGAAATACCGCACGGGTGAGCAAAAACAGG
B MID-36	GTACTGACAGGTGTCACGCTCATGATTTAT
B MID-37	CCTCATACGAGCTGTTTCCTGTGTGGCGTAACAATGATGGATGTGCTCTTGA
B MID-38	CAATATTATTGAAGCATTTTTTGAATCGG
B MID-39	CTAACTCACATTAATTGCGCCTGTCGGGGGAGACTCGCTCGCGAGCG
B MID-40	GCCTTTCTCACGCTGTAGGATAATCAGTTGAG
B MID-41*	**AGACATGAGCGGATACATAATCAGGGGTTG**
B MID-42	CGACCCTGCCGCTTACCGGATACCCTTGGCTCCCTCGTGCTTGG
B MID-43	ACAAATAGGTCAAGGCTTGCGCAAGAAGTGGTCCTGCTTAAAAGTATGCGG
B MID-44	GGCTCGCGTCAAAAAGTGCCGTAAGCGGATGCCGGGA
B MID-45	GCAGACAAGCCCGTCAGGGGGCTTAATTCAGCTGCT
B MID-46	GATACCAGGCGTTTCCCCCTGGAAGGGTGGCGAAACCCGATCGACGCATCT
B MID-47	CGCGCACATACCATTAATCACTCAATAGTGTGCTCATCAAGGATCTTAC
B MID-48	CGGTCGTTCAGAATCATTTTTTTAACAAACAGCTGGCCAGTCACGACGT
B MID-49	GTATCAGCTCACAGCGCTCTTCCGCTTCGGCGGTTAGGA
B MID-50	ACGGTCACAGCTTGTCTACACTGCATACTCAACCTTGGGA
B MID-51	GCATCACAAAAACAGGACTATAAA
B MID-52	ATCATGACATTAACCTCTAAGAATTCCCCGGCGGGTGTTGGGGTTC
B MID-53	GGATAACGCAGGAAAGTATCCACGGCTGCGACTGACTCGCTGCGATCGGCCTTAA
B MID-54	TGAAAACCTCTGACGGCGTAT
B MID-55	CGTTTTTCCATAGGAGGAACC
B MID-56	CACGAGGCCCTTTCGTCACGGTGAGTAATTCTCGGCTTCACTATGCGGCATC
B MID-57	GTAAAAAGGCCGCGTTGCTCTGAAGCGAAGATCAGGGATTGCTCTCCTGTTC
B LEFT-0 handle	CCATCCAGTCTATTAATTGGACACACCTCACACTCCACCTAC
B LEFT-1	TTTTTTGCCGGGAAGCTAGAGTA
B LEFT-2 handle	TGTGCAAAAAAGCGGTTAGCTCCGACACACCTCACACTCCACCTAC
B LEFT-3	TTTTTTCGGTCCTCCGATCGTTGTCAG
B LEFT-4 handle	AAGTAAGGTTGCTCTTGCCCGGCGTCAATAGACACACCTCACACTCCACCTAC
B LEFT-5	TTTTCGGGATAATACCGCGCCACATAG
B RIG-1	TTTTTGCCTGACTCCCCGTCTTCGTTCATCCATAGTTTTT
B RIG-2	TTTTGCTCAGTGGAACGAAAACTTGTCTATGTGTAGA

B RIG-3	CTTTTCTGTATCTGGGCTACACTAGAAGAATTTT
B RIG-4	TTTTCAGTATTTGACGGGGTCTGACTTTT
B LEFT-0 ctrl	CCATCCAGTCTATTAATTGGACCCATCTCTTCTCTCCTCTTC
B LEFT-2 ctrl	TGTGCAAAAAAGCGGTTAGCTCCGACCCATCTCTTCTCTCCTCTTC
B LEFT-4 ctrl	AAGTAAGGTTGCTCTTGCCCGGCGTCAATAGACCCATCTCTTCTCTCCTCTTC
tag β ctrl	TTTTTTTTGAAGAGGAGAGAAGAGATGGGTC
tag β	TTTTTTTTGTAGGTGGAGTGTGAGGTGTGTC

Note: * 5' end was modified with fluorophore Cy5. Highlighted are handles or corresponding dummy sequences.

Supporting References

1. Wood, C. W.; Heal, J. W.; Thomson, A. R.; Bartlett, G. J.; Ibarra, A. Á.; Brady, R. L.; Sessions, R. B.; Woolfson, D. N. Isambard: An Open-Source Computational Environment for Biomolecular Analysis, Modelling and Design. *Bioinformatics* **2017**, *33*, 3043-3050.

2. Marky, L. A.; Breslauer, K. J. Calculating Thermodynamic Data for Transitions of Any Molecularity from Equilibrium Melting Curves. *Biopolymers* **1987**, *26*, 1601-1620.

3. Zhang, P. H.; Too, P. H. M.; Samuelson, J. C.; Chan, S. H.; Vincze, T.; Doucette, S.; Backstrom, S.; Potamousis, K. D.; Schramm, T. M.; Forrest, D.; Schwartz, D. C.; Xu, S. Y. Engineering Bspqi Nicking Enzymes and Application of N.Bspqi in DNA Labeling and Production of Single-Strand DNA. *Protein Expression Purif.* **2010**, *69*, 226-234.

4. Tataurov, A. V.; You, Y.; Owczarzy, R. Predicting Ultraviolet Spectrum of Single Stranded and Double Stranded Deoxyribonucleic Acids. *Biophys. Chem.* **2008**, *133*, 66-70.

5. Douglas, S. M.; Marblestone, A. H.; Teerapittayanon, S.; Vazquez, A.; Church, G. M.; Shih, W. M. Rapid Prototyping of 3d DNA-Origami Shapes with Cadnano. *Nucleic Acids Res.* **2009**, *37*, 5001-5006.